

108
1011
1011

THE HELICAL CONFIGURATION OF
THE POLYPEPTIDE CHAINS IN COLLAGEN

by

Carolyn Cohen

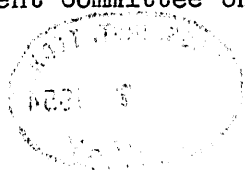
A.B. Bryn Mawr College, 1950

Submitted in Partial Fulfillment of the
Requirements of the Degree of
Doctor of Philosophy
at the
Massachusetts Institute of Technology

Signature of Author _____
Biology Department

Certified by _____
Thesis Supervisor

Chairman, Department Committee on Graduate Students



Biol
Thesis
1954



ABSTRACT

THE HELICAL CONFIGURATION OF THE POLYPEPTIDE CHAINS IN COLLAGEN

Carolyn Cohen
A.B. Bryn Mawr College, 1950

Submitted to the Department of Biology on May 17, 1954, in partial fulfillment of the requirements for the degree of Ph.D.

The following evidence relating to the helical configuration of the polypeptide chains in collagen has been presented in this thesis.

I. It is shown that the polypeptide chains in collagen have a helical configuration in the portions of the protofibril which yield the wide-angle x-ray diffraction diagram.

Diagrams from dry tendon were indexed according to a 28.6 A. period for unstretched material and about a 30 A. period for tendon under tension. Diagrams from moistened tendon have intensity distributions which correspond to the transforms of individual protofibrils.

In order to interpret these diagrams, a treatment was developed based on the theory of Cochran, Crick, and Vand (1952) for helical diffractors. This treatment uses 'helix-nets' and allows a simple analysis of helical diffraction ambiguities.

By application of this analysis, it is shown that the genetic helix in the collagen protofibril has ten scattering nodes in three turns. The genetic helix is the simplest arrangement of equivalent scattering groups and does not necessarily show true chemical connections. Further restrictions on the specific atomic arrangements in the polypeptide chains are derived from the x-ray diagram and from chemical considerations.

A few observations on tendon and long-spacing collagen by small and wide-angle diffraction and electron microscopy support the suggestion that some portions of the collagen protofibril are inaccessible to analysis by wide-angle x-ray diffraction.

II. A polarimetric investigation was carried out for the first time on a soluble, non-denatured, 'pure' collagen fraction (ichthyocol 'procollagen') which had been characterized by physical-chemical measurements (Gallop, 1953, 1954).

'Procollagen' is converted to 'parent gelatin' by heating to temperatures greater than 30°C. At the same time, the specific

Abd. - Oct 3, 1954

rotation ($[\alpha]_D$) changes from -350° to -110° . This change is interpreted as resulting from the loss of a specific collagen configuration in the polypeptide chains of the protofibrils.

'Parent gelatin' gels and shows an increase of specific rotation to about -280° upon cooling. This is the well-known mutarotation phenomenon of gelatin. Rotatory dispersion measurements of 'procollagen' at 11°C ., and 'parent gelatin' at 41°C ., and 2°C ., were obtained at concentrations from 0.02 to 0.3%. These studies combined with information on gelatin films from x-ray diffraction and polarimetry indicate that the mutarotation of gelatin results from the gain and loss of the specific collagen configuration in the polypeptide chains of the gelatin molecules.

III. The conclusions from the wide-angle x-ray diffraction analysis and from the polarimetric study are correlated by the following hypothesis; it is proposed that the high rotation value found in 'procollagen' is due solely to the helical configuration of the polypeptide chains in portions of the protofibril. Consequently, the mutarotation of gelatin is ascribed to the gain and loss of the helical configuration of the polypeptide chains in the gelatin molecules.

It is also suggested that the observed rotation values of globular proteins are related to a random or unfolded configuration of the polypeptide chains in the denatured state, and to a configuration in the native state in which a large cancelling of rotation occurs.

(More detailed aspects of the helical diffraction problem are discussed in the Appendices.)

Thesis Supervisor: Richard S. Bear
Professor of Biophysical Chemistry

Acknowledgement

I wish to thank Professor Richard S. Bear for the invaluable advice he has given me, and for his personal kindness during the past four years. His ideas and influence are evident throughout this thesis.

Thanks are due to Dr. Paul Gallop, and Messrs. Malcolm Rougvie and Harold Wyckoff for many helpful suggestions in the course of this work; and to Dr. Alfred Gierer for discussions on optical rotation.

For instruction in electron microscopy, and for much aid in the preparation of this thesis, I am indebted to Dr. Betty Geren, "whose efforts were none the less arduous for being vain."

The technical assistance of Mrs. John Chow in the optical rotation experiments has been greatly appreciated.

Table of Contents

	Page
Title page	
Abstract	
Acknowledgement	
Table of Contents	
List of Figures	
List of Tables	
Introduction	1
Chapter I: The Structure of the Collagen Fibril	9
A. Experimental data	
1. Small-angle x-ray diffraction data	9
a. Swelling experiments	9
b. KTT under tension	10
2. Investigations of <i>ichthyocol</i> 'procollagen'	12
B. Discussion	14
C. Conclusions	17
Chapter II: Wide-angle X-ray Diffraction Analysis of Collagen	19
A. X-ray diffraction data	
1. Patterns from dry specimens	19
2. Patterns from moist specimens	23
B. Interpretation of the wide-angle diagram	27
1. Helical structure determination by x-ray diffraction	27
a. Basic theory	27
b. Application of the theory to the calculation of transforms	29
c. Application of the theory to the interpretation of the diffraction pattern	31

	Page
(1) Helix geometry	32
(2) Interpretation of the pattern	33
(3) Ambiguities in the analysis	35
2. Application of helical diffraction theory to collagen	38
a. The basic helix-net of collagen	38
b. The structural interpretation of the collagen helix-net	43
C. Conclusions	51
Chapter III: Optical Rotation Studies	52
A. Experimental data	
1. The conversion of 'procollagen' to 'parent gelatin'	53
2. Correlation with viscosity studies	56
3. Rotatory dispersion measurements	60
4. The concentration dependence	65
5. Dependence on ionic strength	67
6. Studies on films	67
7. Summary of experimental data	70
B. Discussion of experimental data	
1. The conversion of 'procollagen' to 'parent gelatin'	71
2. The mutarotation of 'parent gelatin'	73
C. Conclusions	77
Chapter IV: Theories Relating the Rotatory Power and Configuration of Proteins	79
A. The correlation of rotatory power and helical configuration in collagen and gelatin	79
B. An interpretation of the optical rotation of globular proteins	84

	Page
C. Conclusions	98
Summary	99
Suggestions for future work	94
Bibliography	97
Appendix I: Ambiguities of the Helical Diffraction Problem	i
A. The single-cell versus the multiple-cell net ambiguity	i
B. Connection ambiguities	iv
C. The packing of helices	vi
Appendix II: The Optical Transformer	viii
Appendix III: The Calculation of the Fourier Transform of the Coiled-Coil for Collagen	xi
Biography	xvi

LIST OF FIGURES

Figure		Page
1	Small-angle x-ray diagram of KTT swollen in 2.5 M LiCl	11
2	Small-angle x-ray diagram of KTT under tension	11
3	Electron micrograph of ichthyocol 'procollagen' segmental long spacing material	13
4	Wide-angle x-ray diagram of KTT	21
5	Wide-angle x-ray diagram of KTT under tension	21
6	Wide-angle x-ray diagram of KTT, moistened, under tension	21
7	Tracing over Bernal coordinates of x-ray diagram of KTT under tension	22
8	Tracing over Bernal coordinates of x-ray diagram of KTT, moistened, under tension	22
9	Wide-angle x-ray diagram of KTT under tension. Taken with Cu K α radiation.	24
10	Same specimen as in Figure 9 . Taken with Mo K α radiation.	24
11a	'Helix-net', single-cell	33
11b	'Helix-net', multiple-cell	33
12	'Helix-net' for collagen	39
13	Positions of Bessel function maxima for discontinuous helix for collagen	42
14a,b	Projection and optical diffraction pattern for discontinuous helix for collagen	42
15a,b	Projection and optical diffraction pattern for two-strand cable for collagen (Crick, 1954)	50
16	$[\alpha]_D$ versus temperature for different times for ichthyocol	55
17	Ichthyocol, intrinsic viscosity versus specific rotation	58
18	Hide 'procollagen', intrinsic viscosity and specific rotation versus time	58

Figure		Page
19	n_{sp}/c versus concentration for hide 'procollagen' at different times	59
20	Hide 'procollagen', n_{sp}/c versus concentration	59
21	Rotatory dispersion of ichthyocol 'procollagen'. T = 11° C.	62
22	Rotatory dispersion of ichthyocol 'parent gelatin'. T = 41° C.	62
23	Rotatory dispersion of ichthyocol 'parent gelatin'. T = 2° C.	63
24	Rotatory dispersion of ichthyocol in pH 3.7 citrate buffer	63
25	Concentration dependence of specific rotation of ichthyocol 'parent gelatin'. T = 1° C.	66
26	Rotatory dispersion of ichthyocol in 0.05% HAc.	68
27	Rotatory dispersion of 'cold' films of ichthyocol 'parent gelatin'	68

APPENDIX FIGURES

1 a, b	Single-cell 'helix-net' and diffraction pattern	i
2 a, b	Two-cell 'helix-net' and diffraction pattern	ii
3 a, b	'Helix-net' and diffraction pattern	ii
4	Diagram of optical transformer	x
5 a, b	Projection of continuous coiled-coil for collagen, and its optical diffraction pattern	xv
6	Intensity distribution of continuous coiled-coil for collagen	xv

LIST OF TABLES

Table		page
1	Diffraction by dry collagen at wide angles	26
2	Principal near-meridional reflections of dry collagen under tension	26
3	Selection rules and Fourier transforms for helical distributions	30
4	Bessel function orders for discontinuous helix for collagen	40
5	Sources and filters for dispersion measurements	60
6	Representative specific rotation values	64
7	Representative rotatory dispersion constants	64

INTRODUCTION

Collagen has a unique biological and scientific role. It is the most prevalent protein in the animal kingdom. Connective tissue, skin, bone, tendon, and other protective and supporting structures are composed primarily of this material. Collagen is also a protein which is particularly amenable to structure analysis. Information about collagen, therefore, may have implications for other fibrous and globular proteins whose structure is experimentally less accessible.

In the structure analysis of collagen, various levels may be considered. Microscopically visible fibers fray into successively thinner units. One sub-division, called 'fibrils' (Küntzel, 1934), reaches widths near the limit of resolution of light optics. The structural details of the fibrils have been analyzed by small-angle x-ray diffraction (Bear, 1942) and electron microscopy (Schmitt et al., 1942). Within the fibrils are bundles of polypeptide chains, probably running in the direction of the fiber axis. Schmitt et al. (1942) have used the term 'protofibril' to designate the unit of smallest cross sectional area which contains all the molecular properties characteristic of collagen. According to Bear (1952), the width of the protofibril is about 12 A., corresponding to no more than a few, and possibly one, polypeptide chain.

The most powerful optical method to elucidate the configuration of these protofibrils is wide-angle x-ray diffraction. Although much effort during the past 30 years has been devoted to the interpre-

tation of the wide-angle diagram of collagen, only recently has significant progress been made. One of the difficulties is that collagen is a poor diffractor compared with other organic materials. The most characteristic reflections are a 12 Å equatorial spot, a diffuse 4.5 Å equatorial halo, and a sharp 2.86 Å meridional arc. Because of the relatively few and weak reflections, the pattern is not easily analyzed by standard crystallographic procedures. Bear (1952) has described early theories and models proposed for the protofibril.

During the past decade the general concept of helical configurations for the polypeptide chains has been developed. (Huggins, 1943; Bragg et al., 1950). As early as 1943, Huggins had proposed a helical model for collagen. However, this was shown to be unsatisfactory (Bear, 1952). During 1950 and 1951, the results of Pauling and Corey's 'synthetic' approach to the protein structure problems were published (Pauling and Corey, 1950, 1951; Pauling, Corey and Branson, 1951). They proposed specifications for bond angles and distances of amide residues based on crystallographic work with amino acids and peptides. From certain stereochemical rules two helical models, named the α and the γ were derived. In addition, helical models for a number of proteins, including collagen, were proposed. The model they suggested for the collagen protofibril consisted of a helix based on three residues in parallel, and having an axial projection of 2.86 Å per residue. The equatorial structure factor gave excellent agreement with observed intensities on the equator.

In 1952, Bear proposed a different helical model for the collagen protofibril (Bear, 1952). He placed three residues in serial

connection in 2.86 Å.; this accounted for electron optical evidence which suggested that the polypeptide chains were extensible. Stressing the significance of the 20 Å. meridional pseudoperiod which Pauling and Corey had neglected, he accounted for this by placing 21 residues in $\frac{1}{4}$ turns of the helix. The structure was a slightly modified γ helix. The equatorial structure factor for this γ helix model and some variations were calculated by the present author. The helix was found to agree less well with regard to a weak 2.2 Å. equatorial reflection than the three chain model proposed by Pauling and Corey (Bear and Cohen, 1952).

It is of interest to note that because of the difficulties in extracting information from the x-ray diagram, particularly with regard to near-meridional reflections, Huggins, Pauling and Corey, and Bear invoked essentially indirect and independent arguments for the existence of the helix in collagen. Thus, information from stereochemistry and electron microscopy was of major importance in the development of the helical concept for the collagen protofibril.

In 1952, Cochran, Crick and Vand published their work on the Fourier transforms of helical diffractors. From the treatment they derived, the interpretation of near-meridional intensities from helical diffractors could be made. In this thesis, an analysis which indicates that collagen is a helical diffractor is developed directly from the x-ray diagram. Basic specifications for the helix are also presented. In addition, some new wide-angle x-ray diffraction data are given. A brief note (Cohen and Bear, 1953) has already been published at an earlier stage of the analysis.

The other part of this thesis describes the application of polarimetry to determine the configuration of the polypeptide chains in collagen. Optical activity allows a sensitive measurement of short-range structural detail, and, thus, complements the wide-angle x-ray diagram. In addition, polarimetry permits the analysis of material in solution. However, it is a more formidable method than x-ray diffraction from the point of view of interpretation. Since the classical work of Fresnel (1825), Pasteur (1848) and van't Hoff (1875), progress has been slow in attempts to correlate molecular structural with optical activity. Many of the useful results of polarimetry studies in the past have been based on empirical rules of optical rotation. Thus the van't Hoff principle of superposition was used by Hudson (1909) to derive the structure of sugars. Modern theoretical treatments are given in papers by Kuhn (1930), Condon (1937), Kirkwood (1937), Kauzmann, Walter and Eyring (1940). Such theories permit the prediction of the sign and value of rotation only for very simple molecules.

For molecules as complicated as proteins, even an empirical approach has been neglected. In recent years, however, optical rotation has been used as a criterion for detecting the occurrence of configurational changes in proteins (see, for example, Jirgensons, 1950, 1951, 1952 a,b). Since the present state of knowledge of protein structure, while rapidly advancing, is still very incomplete, correlation of rotations with protein configuration has been vague (Doty and Geiduschek, 1953; Kauzmann et al., 1953; Yang and Foster, 1954).

Gelatin, the degradation product of collagen, has proved to be especially suitable for analysis by polarimetry. It is a very soluble material with a high specific rotation, and undergoes a well-known and

striking mutarotation phenomenon. When gelatin is cooled and changes from the sol to the gel state, the specific rotation more than doubles, going from about -120° to -300° and this change is reversible (Trunkel, 1910; Smith, 1919).

The fact that aggregation occurs as a gelatin sol is cooled has led some investigators in the past to attribute the rotation change to this effect (Kraemer and Fanselow, 1925). The proof of aggregation in solutions too dilute to form stiff gels is seen from the increase of viscosity and turbidity of these solutions upon cooling (Boedtker, 1953).

However, as long ago as 1919, Smith (on the basis of questionable experimental data) suggested that two different molecular species exist in the sol and the gel. The classical work of Katz proved that such a configurational difference did in fact exist. He found that a gelatin sol, either wet in a capillary, or evaporated to form a film at a temperature greater than 40° C, gives an amorphous type x-ray diagram in which the 2.86 A. reflection characteristic of collagen is missing. The 10 A. reflection is present but diffuse. However, he found that gelatin gel, either wet or evaporated to form a film, yields the 2.86 A. reflection, and the 10 A. reflection is sharpened. (Katz, Derksen and Bon, 1931; Katz, 1932; Derksen, 1932; Katz and Derksen, 1932) The appearance of the 2.86A.spacing can only mean that there is a change in the configuration of the sol upon gelling and that this change is due to the formation of the characteristic collagen configuration in the polypeptide chains.of the gelatin molecules.

Katz' own interpretation was that the two species proposed by Smith corresponded to an amorphous (hot gelatin) form and a crystalline

(cool gelatin) form, and that the latter was similar to collagen.

More recent work has tended to favor the importance of the configurational effect. Thus, from studies on the concentration dependence of mutarotation, Ferry proposed that intramolecular changes were the principal factor in causing mutarotation (Ferry and Eldridge, 1949). The work of Robinson has given the most specific correlation of configuration with rotation (Robinson and Bott, 1951; Robinson, 1953). He found that films made from drying 'cold' gelatin had a high specific rotation ($[\alpha]_D \simeq -1000^\circ$), and exhibited infrared absorption characteristic of collagen. Films made from 'hot' solutions of gelatin showed the absorption corresponding to an α or β configuration of proteins, and these films had a specific rotation of about -125° . From this work Robinson has ascribed the changes in rotation of solutions of gelatin to the gain or loss of the specific 'collagen fold' of the polypeptide chains.

It should be stressed that in the past no comparison was made of the optical rotations of collagen and of gelatin, although the wide-angle x-ray diagrams as well as the infrared absorption of these two systems were compared. The work of Thureaux (1945) on the rotation of acid extracts of collagen is an exception, but the impurity of the systems she examined prevented quantitative conclusions. Thus, the specific rotation of a 'pure' collagen preparation was not available for use as a standard of reference in the molecular interpretation of the mutarotation phenomenon.

In 1948, Orekhovitch et al. (1948 a,b) published their work on a 'pure' soluble fraction of collagen which they called 'procollagen.' This material has been studied by other investigators (Bresler et al., 1950;

Randall et al., 1952).

In 1953, Gallop, in this laboratory, obtained 'procollagen' from ichthyocol and characterized, by physical-chemical methods, both this material and the gelatin produced from it. By light scattering and sedimentation he has shown that the unheated 'procollagen' is probably a polydisperse system of weight average molecular weight about $1-2 \times 10^6$. He presented evidence that these units correspond to the 'protofibrils' of collagen. Using the Peterlin analysis of light scattering and sedimentation data, he found an average contour length of about 13,400 A. and mass per unit length of about 80-120 avograms per A. When this material is heated to 40° C., a complete conversion takes place, yielding a monodisperse system of particles of molecular weight 70,000 (as determined by diffusion and light scattering). This product has been called 'parent gelatin' by Gallop (1953, 1954) and that terminology will be maintained in this thesis. Analysis of data from viscosity, sedimentation and diffusion studies gives an effective length (root mean separation of chain ends) of 225 A. for the 'parent gelatin' molecule, if it is treated as a random coil; if it is characterized as a prolate spheroid, the dimensions are about 20 x 400 A.

The present author has studied the optical rotation of 'procollagen' and its derived gelatin. For the first time a 'pure' fraction of undegraded collagen, and a monodisperse gelatin were used in investigating the mutarotation phenomenon. In addition, the optical rotation and rotatory dispersion of gelatin at concentrations lower than any reported previously have been measured. The results of these studies are presented in this thesis and an interpretation on a molecular basis is given for the observed optical rotation changes in

'procollagen' and 'parent gelatin'.

In the final chapter of this thesis an hypothesis is formulated which relates the conclusions drawn from the x-ray diffraction and optical rotation analyses. The author suggests a correlation of the helical configuration of the polypeptide chains with the rotation values observed in 'procollagen' and 'parent gelatin'. In addition, theories are suggested which relate the optical rotation and configuration of globular proteins in the native and denatured states.

CHAPTER I

The Structure of the Collagen Fibril

Wide-angle diffraction and polarimetry are methods which give information about the protofibril at a structural level of atomic dimensions. Knowledge of higher structural levels in collagen is necessary for the proper interpretation of data obtained by these methods. Evidence from electron microscopy and small-angle x-ray diffraction is valuable in establishing the structural identity of material studied by the higher resolution optical techniques. Furthermore, such evidence is of aid in determining whether the wide-angle diagram of collagen characterizes all, or only a portion of, the protofibril. This fact is important for the analysis of protofibrillar structure. It is also of significance in the correlation of optical rotativity with protofibrillar structure, since the specific optical rotation of a substance relates to the entire structure.

In the following section a few experiments which are relevant to these questions are reported and briefly discussed.

A. Experimental data1. Small angle x-ray diffraction studies of tendon

The two small-angle cameras used in this investigation have been described by Bolduan and Bear (1949). The cameras had pin-hole collimation which allowed a resolution of 200 x 400 A. for one camera, and 400 x 800 A. for the other, at about 15 cm. Filtered Cu K α radiation was used.

a. Swelling experiments

The swelling of tendon at neutral pH's was investigated by small-angle x-ray diffraction. The water uptake of kangaroo tail tendon

(hereafter, KTT) was determined as a function of the concentration of LiCl, LiBr, and LiI. The swelling effects of the reagents increased in that order. KTT samples (about 6 inches in length) were soaked in distilled water, and stretched under high tension, until dry. Short lengths of tendon, less than 1 mm. in diameter, were placed in thin walled glass capillaries and various concentrations of LiCl were added. LiCl was used since this had the smallest x-ray absorption coefficient and also produced a large swelling effect. (KTT in 2.5 M LiCl absorbed more than twice as much water by weight as KTT in distilled water.) The tubes were sealed with a flame and the ends coated with paraffin.

The small angle diagrams obtained were similar to those yielded by KTT swollen with distilled water. (Bear, 1942; Bear, 1952; Rougvie and Bear, 1953). See Figure 1. The diagram has sharp meridional reflections with odd orders strong and even orders weak. Periods ranged from 673 Å. with distilled water, to 654 Å. with 2.5 M LiCl.

The wide-angle diagram of KTT in 2.5 M LiCl showed the characteristic 2.86 Å. reflection.

b. KTT under tension

KTT was stretched by a method described in the section on wide-angle diffraction (p. 20). The sample was irradiated while under tension in the small-angle camera. Figure 2 shows a pattern obtained from a sample which had a 700 Å. period. The meridional reflections are sharp with odd orders strong and even orders weak. This is very similar to the pattern from the hydrated specimen shown in Figure 1. The pattern obtained from the most highly stretched specimens had a period of about 703 Å. and showed only 4 orders, of which the second and

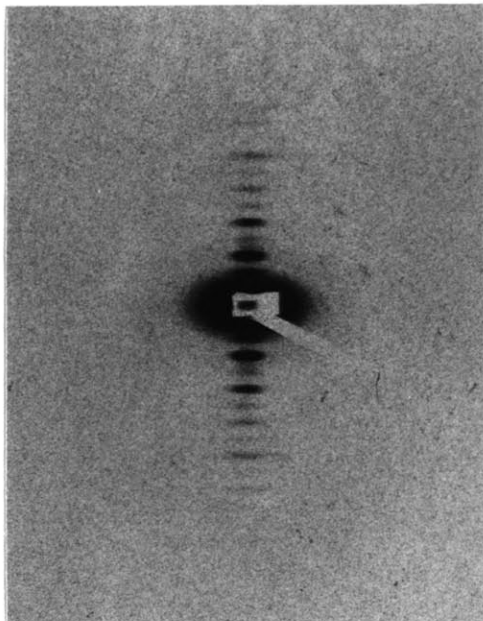


Figure 1
Small-angle x-ray diagram of
KTT swollen in 2.5 M LiCl

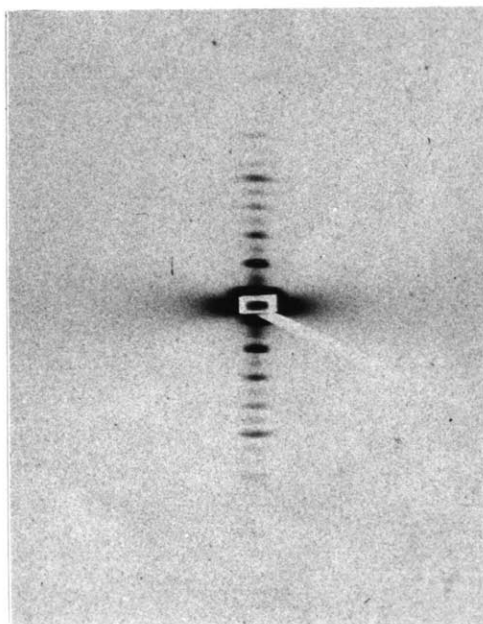


Figure 2
Small angle x-ray diagram of
KTT under tension

the third were almost equally intense.

The wide-angle diagrams of these highly stretched tendons showed an increase in period which is discussed below.

2. Investigations of ichthyocol 'procollagen'

Solutions of ichthyocol 'procollagen' prepared by citrate extraction as described by Gallop (1953), were dialyzed against phosphate buffer (pH 8) or tap water and the precipitate examined with the electron microscope. Typical collagen fibrils with the 640 A. period were seen.

Following the directions of Schmitt et al. (1953) 0.2% solutions of ichthyocol 'procollagen' in 0.05% HAC were dialyzed in the cold against an equal volume of 0.4% ATP (free acid). The resultant precipitate was fixed with phosphotungstic acid and examined with the electron microscope. The precipitate was found to consist almost entirely of 'segment long spacing' units (Figure 3). These results were reproducible with other preparations of the ichthyocol 'procollagen.' The length of the segments was about 1800 A. The widths varied from thin segments to wider ribbon-like strips. Films of this material gave poorly oriented, collagen wide-angle diagrams. Schmitt et al. (1953) have previously reported the same results with x-ray patterns of long spacing material.

When cool 'parent gelatin' in 0.05% HAC was dialyzed against 0.4% ATP, a light thermolabile precipitate was formed. This precipitate dissolved upon reaching room temperature and reprecipitated when the solution was cooled. Only a part of the 'parent gelatin' is involved in this reaction since the same concentration of unheated 'procollagen'

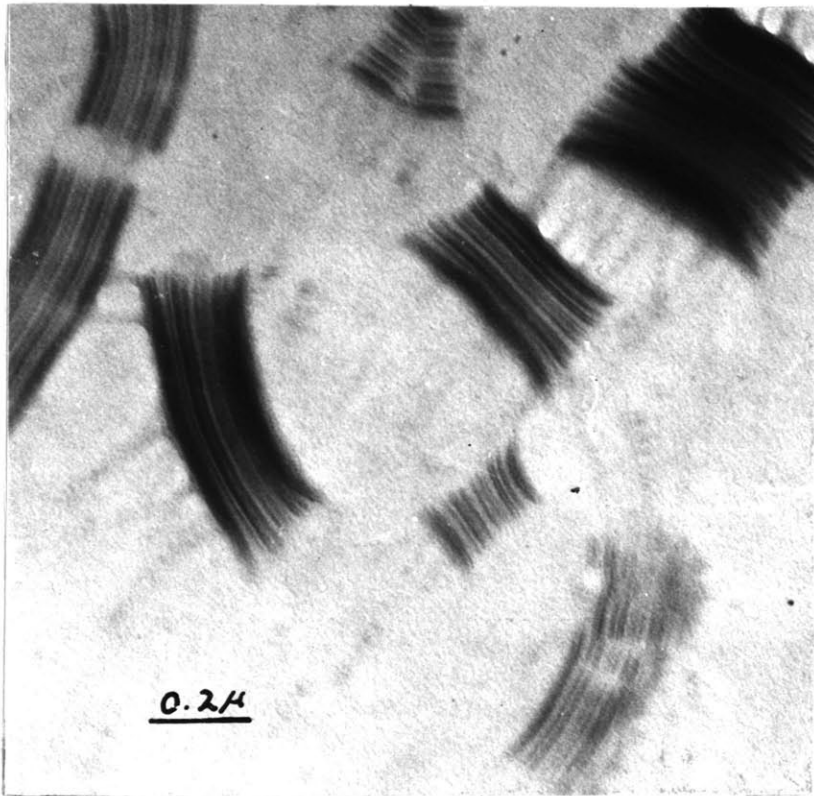


Figure 3

Electron micrograph of segmental long spacing precipitate of ichthyocol 'procollagen' dialyzed against ATP. Stained with PTA.

yields a much more copious precipitate. Films of the ATP-parent gelatin precipitate prepared in the cold yielded the collagen wide-angle diagram. Electron microscope pictures of this material fixed with osmium tetroxide or phosphotungstic acid showed amorphous fibrous masses.

B. Discussion

1. Small angle studies of tendon

Bear (1952) has summarized the evidence from small-angle x-ray diffraction that within the 640 A. period of collagen there are regions of order (interbands) and regions of disorder (bands).

The band-interband concept of structure was derived from the characteristic fanning which is exhibited by meridional orders in patterns from dry tendon. This is especially marked in KTT. In patterns from moist tendon (with periods up to 670 A.), the layer lines do not show fanning (Bear, 1942). The interpretation of the pattern from moist tendon was that band distortions are decreased by the addition of water and this leads to the loss of fanning.

An intensity distribution of odd orders strong and even orders weak is found in patterns from moist tendon. This was interpreted to mean that in the wet specimen a cosinusoidal variation of electron density occurred along the fibril. Roughly half the period had greater than average electron density, and half had less than the average electron density (Bear, 1942). Because of the complication of water the extrapolation of this aspect of the structure to the dry fibril was not made.

This new evidence represents the first high resolution small-angle diagrams of tendon under tension. These show that dry tendon under high tension not only loses fanning, but has a variation of electron density similar to that of hydrated specimens. This may be interpreted to mean that both water and tension increase the intrafibrillar orientation, thus permitting the appearance of this electron density variation.

Data from electron microscopy are consistent with this concept. Shadowed preparations and many stained and unstained preparations show a 'scalloped' appearance along the fibril. This corresponds to the cosinusoidal variation of electron density dividing the period into halves as predicted from the small-angle x-ray diffraction data. It should be noted, moreover, that both bands and interbands are present in each half of the period.

Very high tensions will eventually have the effect of wiping out the intensity of higher orders as slippage occurs within the fibrils. This may explain the decrease of intensity in the third order relative to the second which was observed in one pattern.

The loss of fanning and intensity changes which occur in the small-angle diagram, without corresponding changes in the wide-angle diagram, are data supporting the suggestion by Bear (1942, 1952) that the wide-angle diagram relates only to portions of the protofibrils.

2. Experiments on ichthyocol 'procollagen'

Two kinds of long-spacing modification have been described for collagen (for references, see Schmitt et al., 1953). One is a

'fibrous long spacing' material which can be formed by the addition of mucoprotein to acetic acid extracts of swim bladder. The periods range from 1800 to 3000 A. in length and are unpolarized. The other kind is 'segmental long spacing' which can be formed by the addition of ATP to similar extracts. Two different sizes of polarized segmental units are formed depending upon the source and method of extraction. One is about 1800 A. long and the other about 2500 A. The ability to reconstitute these long spacing structures may be considered a criterion for the identification of collagen.

Gallop (1953,1954) has described x-ray diffraction and electron microscope data which characterize ichthyocol 'procollagen' structurally as a 'typical' collagen. On the basis of solubility, however, this material is classified as a particular fraction of collagen. The data presented above show that the ichthyocol 'procollagen' fraction is able to form the 'segment long spacing' modification.

In addition, the fact that the 2.86 A. reflection persists in the wide-angle diagrams of such materials means that at least some of the collagen protofibril remains intact during the conversion to long-spacing material.

'Parent gelatin' does not seem to reconstitute material showing large structural periods. The intramolecular configuration of 'parent gelatin' described later in this thesis, can account for these results.

3. The collagen molecule

We may briefly summarize an interpretation of the molecule which is consistent with the experimental data. Bear (1952) has

suggested that the collagen molecule has a length of 640 A. along the protofibril. He also proposed that this unit uncoils to form the long-spacing modifications. Since the wide-angle diagram (chiefly the 2.86 A. spacing) persists in the long-spacing modifications, this may mean that the uncoiled protofibrils, perhaps by some rearrangement, can yield this diagram. Or, the unfolding concept may be revised to specify that only some portions of the protofibril change in the conversion to long-spacing material. The bands may be the regions of the protofibrils which take part in this conversion. There is evidence that the bands do not contribute greatly to the collagen wide-angle diagram (Bear, 1952) and any configurational changes they undergo would not be detected by this method. In addition, Bear has suggested that the amino acids with side chains carrying polar groups are localized within the bands. These would be expected to react with reagents causing long-spacing modification. However, a serious difficulty with such a picture is that if only the bands uncoil, the three-fold increase of period would have to be accounted for by a large difference in the amount of material in the bands and interbands. At present, the relative proportion of material in these regions is not known. The two different long-spacing modifications may both be produced from the polarized 640 A. particle. It might be imagined that in the presence of ATP the polarized long-spacing particle is oriented in one direction only, whereas with mucoprotein acting as a cementing substance, the long-spacing particle is oriented in both directions and forms an unpolarized unit (See Schmitt et al., 1953).

C. Conclusions

1. Small-angle diagrams of dry tendon under tension supplement

previous studies on hydrated tendon, and reveal that a fundamental property of the collagen fibril is a cosinusoidal variation of electron density. The period of from 640 to 700 A. is about equally divided into a region having greater than average electron density, and one with less than average electron density, the division being roughly in the middle of the period.

2. An ichthyocol 'procollagen' fraction, used in the polarimetry investigation described below, is a 'typical' collagen in its ability to form long-spacing material.

3. The experimental results which show changes occurring at small angles, without corresponding changes at wide angles, support the concept that portions of the protofibrils are inaccessible to analysis by wide-angle x-ray diffraction.

Chapter II

Wide Angle X-Ray Diffraction Analysis of Collagen

A. X-ray diffraction data

The collagen wide-angle pattern consists of three strong near-meridional reflections at spacings of 9.55, 3.76, and 2.86 Å., and a strong equatorial reflection at about 11-12 Å. A very characteristic feature also is the diffuse 4.5 Å. equatorial halo.

A more detailed description follows.

1. Patterns from dry specimens

Figure 4 shows a pattern obtained from KTT, with fiber axis normal to the beam of filtered Cu K α radiation. Higher angle meridional reflections were obtained by the use of a cylindrical camera (radius 4.7 cm) with specimens tilted at appropriate angles to the beam. Oscillation photographs were also taken. In addition to KTT, rat tail tendon, tunic from carp swim bladder (ichthyocol), and demineralized mammoth tusk were examined. These materials gave similar high angle meridional reflections except that the 2.3 Å. spacing (which is very weak for KTT) was not observed. The observed spacings and approximate intensity relationships for KTT are listed in Table 1. Some of these spacings (with one change) have been reported previously (Cohen and Bear, 1953). Arcing and diffuseness of the higher order reflections lead to the uncertainty noted in the table. All near-meridional reflections smaller than 2.86 Å. were measured as meridional. Meridional indices were assigned on the basis of a 20 Å. pseudoperiod in Bear (1952) and Cohen and Bear (1953). Although this is the smallest period which accounts for the data, it is also an approximation. The larger

and more exact period is 28.6A. However, helical diffraction theory shows that basically similar structures are prescribed by the two periods (see page 38). In Table 1 indices are assigned according to the 28.6 A. period. Reflections obtained with Mo K α and reported by Perutz (1952) are also included in the table.

The pattern shown in Figure 4 may be considered the 'classical' collagen diagram. It was obtained by moistening the KTT and allowing it to dry under tension. Then the fiber, released from tension, was irradiated. In 1953, Cowan reported the work of North who obtained patterns from rat tail tendon under high tension. Spacings up to 3.1 A. were observed for the 2.86 A. reflection (Cowan et al., 1953). Attempts were made by the present author to duplicate these results. Both KTT and beef tail tendon were examined. In order to avoid the shearing caused by clamps, the stretcher consisted of two opposing bars slotted at the end, one of which could be moved by a fine adjustment. The ends of the tendon were pulled through the slots and wrapped around the bars. Tendon was stretched in both wet and dry condition and irradiated while under tension in the stretcher. The highest spacing obtained for the 2.86 A. reflection was 2.96 A. Figure 5 shows a pattern from dry KTT under tension. Figure 7 shows the tracing over Bernal coordinates of a similar pattern. In the patterns obtained from all specimens, the three prominent near-meridional reflections maintained their indexing relationships within the accuracy of the measurements (see Table 2). A correction should be added to ^{the} 4.2 A. spacing (and a smaller one to the 2.95 A. spacing) to account for the curvature of the sphere of reflection. This makes the true period closer to 30 A.

Some other differences between the patterns in Figures 4 and 5 are the decrease of meridional versus near-meridional intensity of the third and seventh layer lines, in Figure 5. This splitting of the

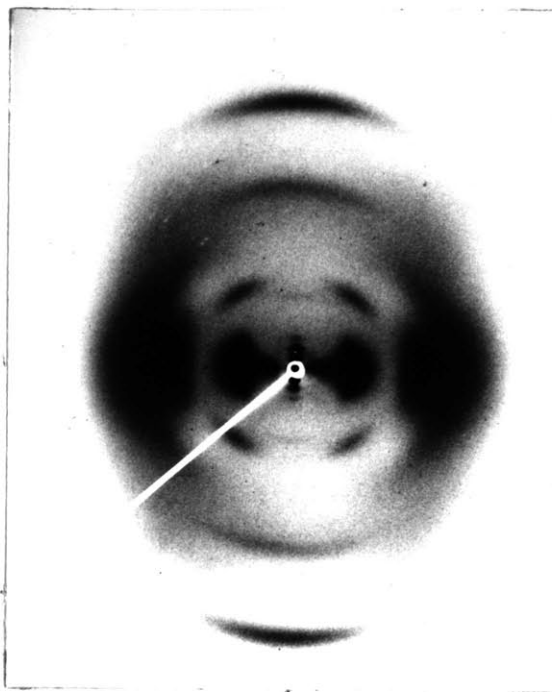


Figure 4

Wide-angle x-ray diagram of KTT

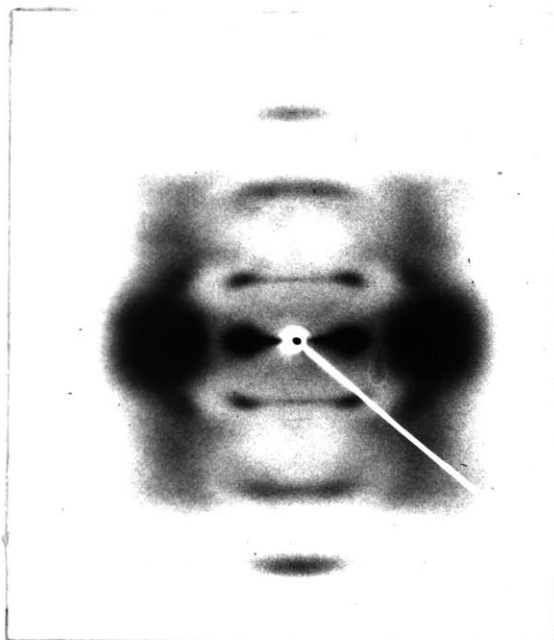


Figure 5

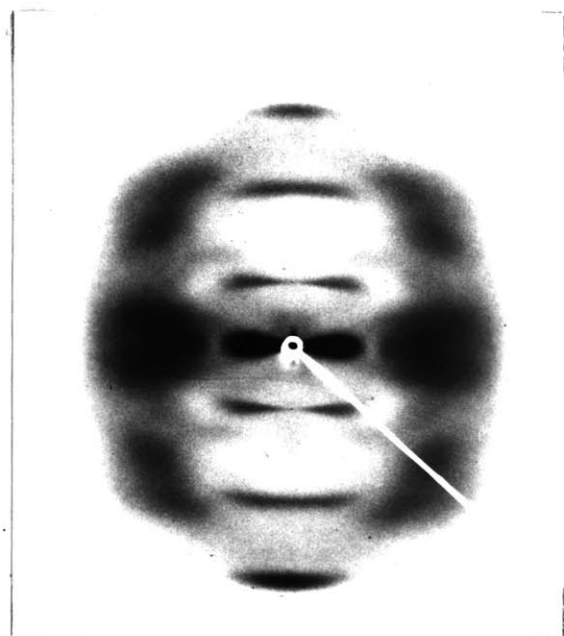
Wide-angle x-ray diagram of KTT
under tension

Figure 6

Wide-angle x-ray diagram of KTT
moistened, under tension

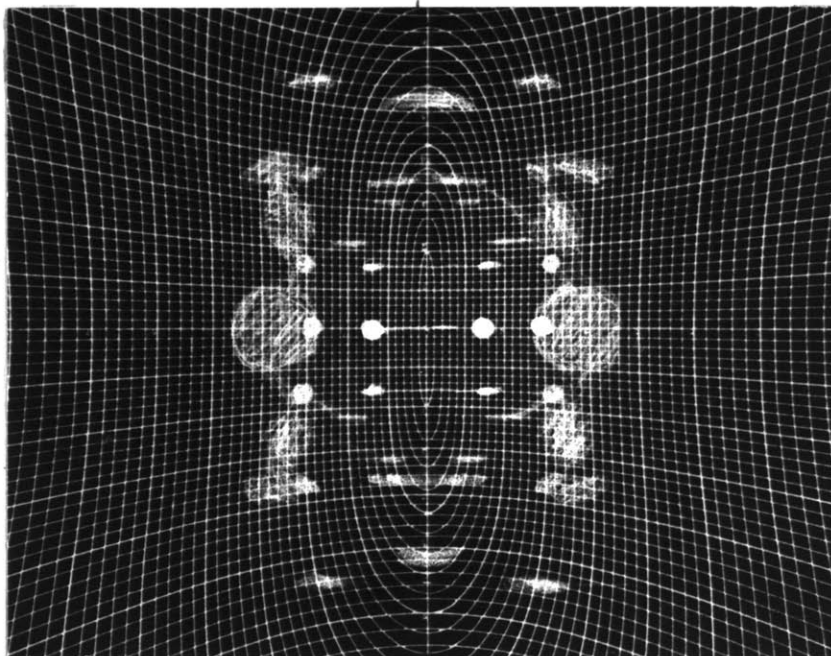


Figure 7
Tracing over Bernal coordinates (flat film, 5.0 cm.
specimen to film distance) of x-ray diagram of
KTT under tension

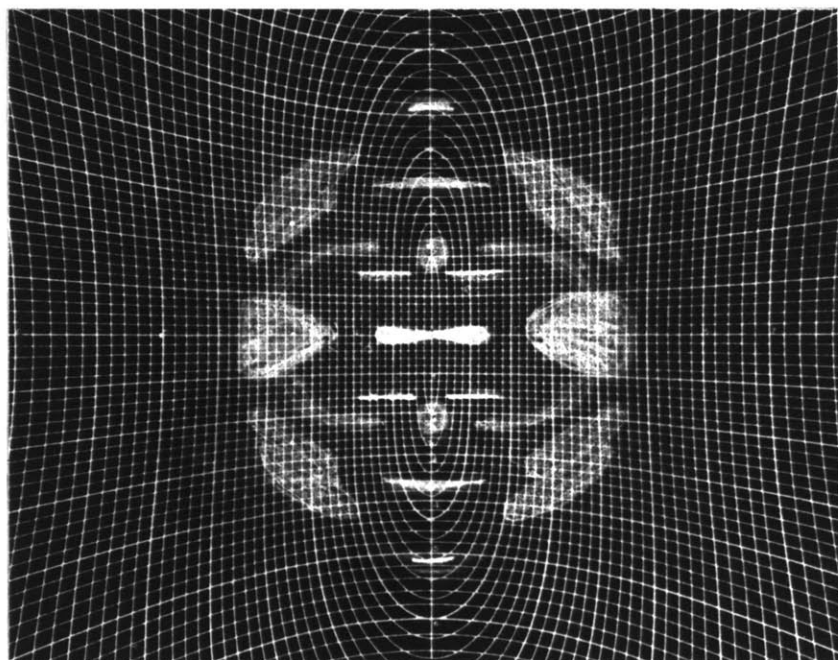


Figure 8
Tracing over Bernal coordinates (flat film, 5.0 cm.
specimen to film distance) of x-ray diagram of
KTT, moistened and under tension.

third and seventh layer lines indicates that these are not true meridional reflections. There is also an apparent decrease of intensity of the 2.95 Å. reflection relative to the 9.7 Å. reflection.

Mo K α radiation was used to test whether this latter intensity change is due to the fact that in the highly stretched fibers less of the specimen is tilted into the sphere of reflection than in the case of the more poorly oriented fibers. Mo K α radiation has a smaller curvature of the sphere of reflection than Cu K α , and enables the true intensity relationships of the reflections in question to appear. Figure 9.10 shows a comparison of the same stretched sample of KTT irradiated with Cu K α and Mo K α . It is seen that the correct intensity relationship is similar to that in Figure 4'.

It is clear that Figure 5 is a 'better' diagram than Figure 4' because of the decrease in arcing in the pattern. However, it is not the most useful diagram for determining the transform of an individual diffracting unit, the protofibril, since as seen in Figure 7, the transform is clearly sampled by a poorly developed lattice.* The sampling observed is consistent with that expected for hexagonal packing of cylinders. The distance between cylindrical diffracting centers is about 12 Å. in unstretched samples at normal humidity, and about 10-11 Å. in stretched samples.

2. Patterns from moistened specimens

Figure 6 shows a pattern obtained from moistened KTT under tension. The tendon was kept moist while in the stretcher by means of

* By this we mean that packing arrangements result in intensity being permitted only at reciprocal lattice positions. Thus, in effect, we can think of the continuous transform of the individual diffracting unit as being 'sampled' at these discrete positions.

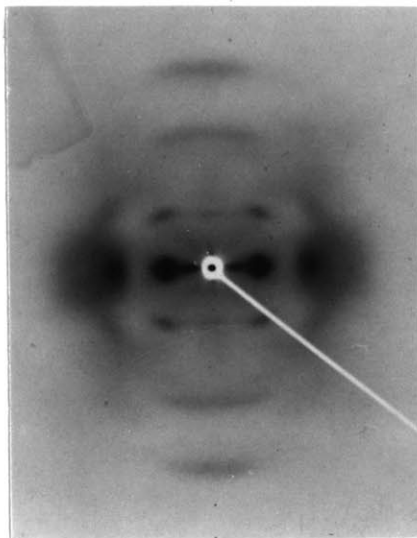


Figure 9

Wide-angle x-ray diagram
taken with Cu K radiation
of KTT under tension

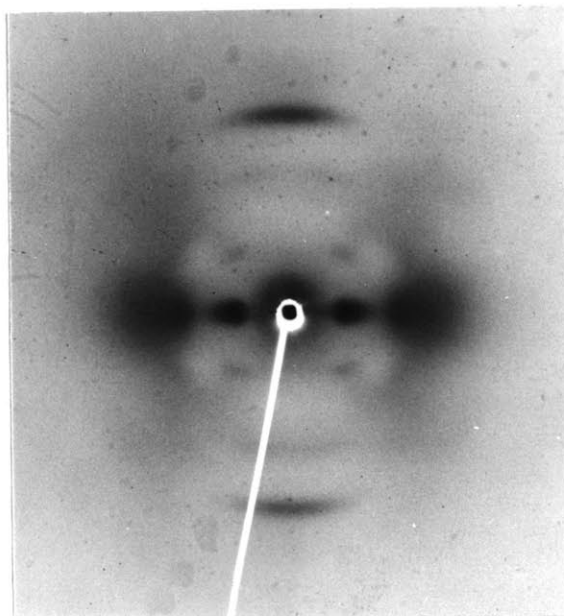


Figure 10

Wide-angle x-ray diagram
taken with Mo K radiation
of same specimen as in Figure

wet filter paper in which windows were cut to allow the x-ray beam to hit only the specimen. From Figure 6, it is seen that most of the lattice has been eliminated by the treatment with water, and the unsampled intensity relationships are available. This is the pattern whose intensity distribution must be explained by any model. One should remember, however, that the presence of water changes the ratio of the protein to background electron density.

Figure 8 shows a similar pattern traced over Bernal coordinates. In patterns from moistened specimens in which the lattice is still present the strong equatorial row line reaches spacings up to 16 Å. (Küntzel and Prakke, 1933). As the specimen is dried, the spacing decreases to a lower limit of about 10.6 Å. in unstretched tendon (Rougvie and Bear, 1953) and less than this in stretched tendon (Cowan et al, 1953).

It may be noted that a spread of diffuse intensity shows up in Figure 6 at close to the correct value for ~~the fourth layer line~~. This spacing has a meridional component also. No such intensification is apparent in dry specimens (Figure 5). In addition, intensity seen on the sixth layer line in patterns from dry specimens (see Figure 5) seems to have disappeared in patterns from moistened specimens.

From Figure 6, it is seen that two kinds of diffraction may be distinguished on the collagen wide-angle diagram. The strong near-meridional reflections are confined relatively sharply to the third, seventh, and tenth layer lines. On the other hand, a diffuse row line at about 4.5 Å. is composed of diffractions not clearly located on layer lines. The greater distance of these diffractions from the meridian accounts for some of the diffuseness.

Table 1

Diffraction by Dry Collagen at Wide-Angles

Near-Meridional

Observed Spacing	Relative Intensity	Layer Line Index	Period $c = \lambda d, \text{A.}$	Bessel Function Order n
(∞)	--	0	----	--0--
9.55	S	3	28.7	1
3.97	S	7	27.8	1
2.86	VS	10	28.6	0
2.54	W	11	27.9	3
2.3	VW	13	30.	1
2.06	W	14	28.8	2
1.84	W	16	29.4	2
1.64	W	17	27.8	1
1.44	W	20	28.8	0
0.98*		30	29.4	0
0.76*		40	30.4	0
0.60*		50	30.0	0

Equatorial

Observed Spacings, d, A.				and Relative Intensity
11.6 VS	5.7 S	4.6 S	2.25 \pm .05	W [†]

* Reflections obtained with Mo K α and reported by Perutz (1952).

† May not be true equatorial reflection, since off-equatorial components appear to be strong.

Table 2

Principal Meridional Reflections of Dry Collagen Under Tension

Observed Spacing d, A.	Layer Line Index	Period $c = \lambda d, \text{A.}$
9.97	3	29.9
4.18	7	29.3
2.95	10	29.5

B. Interpretation of the wide-angle diagram

The history of the problem has been outlined in the introduction. In the next section the necessary helical diffraction theory is presented with particular emphasis placed on ambiguities encountered in the analysis. In the subsequent section the theory is applied to the collagen wide-angle diagram.

1. Helical structure determination by x-ray diffraction

Introduction

The helical diffraction problem may be approached systematically. The plan of this discussion is to consider first the diffraction from certain mathematically 'ideal' helical distributions. Basic theory, including the necessary Fourier transforms and selection rules, will be developed in this section. Application of the theory to the interpretation of the diffraction diagram will then be discussed. The analysis will finally deal with ambiguities encountered in the structure determination.

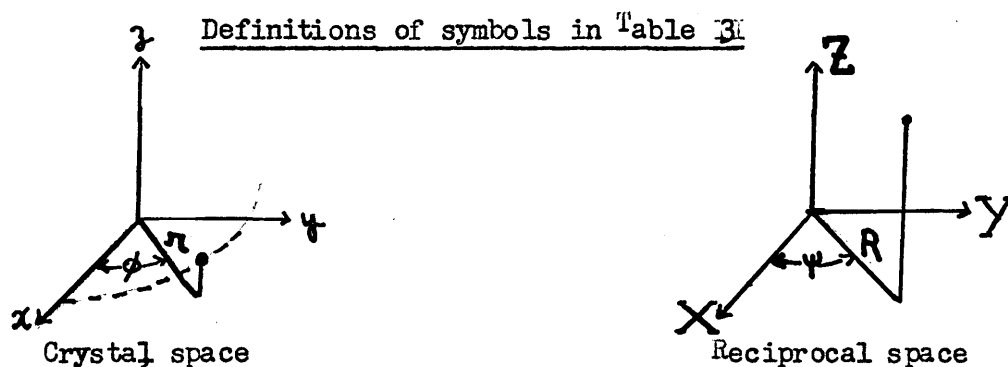
a. Basic theory

The Fourier transforms for certain helical diffractors have recently been derived by Cochran, Crick and Vand (1952) and Crick (1953a).

Definitions: Three kinds of distribution are considered:

1. The continuous helix is defined as a uniform helical scatterer infinitely thin and long.
2. The discontinuous helix is a periodic set of points on a continuous helix; scattering takes place from these points only.
3. The coiled-coil is either 1. or 2., in which the axis of the helix itself forms another helix.

The discontinuous coiled-coil is the most general array; all other distributions may be considered as special cases of this. The selection rule for the Fourier transform of a discontinuous set of points arranged on a coiled-coil has been derived by Crick (1953a). By appropriate conditions the selection rules and transforms of other distributions may be derived from this. Table 3 presents this information.



Coordinate Systems

N_0 = number of turns in major coil

N_1 = number of turns in minor coil

r_0 = radius of major helix

r_1 = radius of minor helix

ϕ_0 = angular coordinate of major helix

ϕ_1 = angular coordinate of minor helix

ϕ_m = angular coordinate of scattering center

z_0 = initial z coordinate of major helix

P = repeat of major coil

C = period = $N_0 P$

λ = layer line index

n, m', p, q, d, S = any integer

M = number of scattering centers

$$\tan \alpha = 2\pi r_0/P$$

$$\bar{r}_1 = r_1 (1 + \cos \alpha)/2$$

$$\Delta = r_1 (1 - \cos \alpha)/2$$

b. Application of the theory to the calculation of transforms:

For the purposes of analysis, any helix consisting, for example, of groups of amino acid residues acted upon by a screw axis or axes, may be reduced to one of the configurations considered above. Variations of electron density due to the atomic discontinuities may be 'smeared out' and a continuous helix used as a representation. Marked discontinuities of electron density, corresponding to the repeat of each amino acid residue, or to the scattering from a particular side chain sequence, may be condensed to a periodic distribution of nodes, or point centers of scattering. Diffraction from such distributions (considered independently, or packed in various ways) may be analyzed by the preceding transforms. This enables rapid model evaluation. It is clear, however, that although the transform obtained in this way is correct, it is incomplete. The complete expression for the structure includes the transform of the electron density distribution about the node, and within the 'continuous' electron density 'smear.'

Examples of some transform calculations are given in this thesis. They are based on the analysis of the collagen diagram. The simplest case is that of the discontinuous helix, calculated from equation 5^a. This is presented on page 40. The calculation of the transform of the continuous coiled-coil according to equation 3 is more difficult. Both the methods and the results of such a calculation are given in Appendix III.

Tab. 3

Fourier Transforms and Selection Rules for Helical Distributions

<u>Conditions</u>	<u>Selection Rule</u>	<u>Transform</u>
	$N_0 p + (N_1 - N_0) q + N_1 s + (N_0 + N_1) d = \ell + M m'$	$\sum_p \sum_q \sum_s \sum_d J_p(2\pi R r_0) J_q(2\pi R r_1) J_s(2\pi(\ell/c)r_1) \times e^{[ip(\psi - \phi_0 + \pi/2) + iq(-\psi + \phi_1 + \pi/2) + i(\phi_m + 2\pi i \ell z_0/c)]}$
$\Delta \rightarrow 0$ $d = 0$	$N_0 p + (N_1 - N_0) q + N_1 s = \ell + M m'$	$\sum_p \sum_q \sum_s J_p(2\pi R r_0) J_q(2\pi R r_1) J_s(2\pi(\ell/c)r_1) \times e^{[ip(\psi + \phi_0 + \pi/2) + iq(-\psi + \phi_1 + \pi/2) + i(\phi_m + 2\pi i \ell z_0/c)]}$
$m' = 0$	$N_0 p + (N_1 - N_0) q + N_1 s + (N_0 + N_1) d = \ell$	<p>Same as 1. with $m' = 0$.</p>
$\Delta \rightarrow 0$ $m' = 0$	$N_0 p + (N_1 - N_0) q + N_1 s = \ell$	<p>Same as 2. with $m' = 0$.</p>
$N_1 = 0$	$N_0 n_1 = \ell + M m' \quad (a)$ $(M - N_0) n_2 = \ell + M m'_2 \quad (b)^*$ (where $n_1 = -n_2$)	$\sum_n J_n(2\pi R r) \exp [i n (\psi + \pi/2)]$
$N_1 = m'$ $= 0$	$N_0 n = \ell$	$J_n(2\pi R r) \exp [i n (\psi + \pi/2)]$

ved by a substitution.

For the calculation of structure factors, the groups of amino acid residues are broken up into sets of like atoms, each set being at a certain radius from the central axis. These sets are then treated by a simple extension of the methods derived for the discontinuous helix (Cochran, Crick, and Vand, 1952).

c. Application of the theory to the interpretation of the diffraction pattern

If a pattern can be indexed according to any of the selection rules listed in the preceding section, the helical nature of the diffractor is possible and the basic aspects of structure may be specified. In the usual crystallographic case, the symmetry properties of the diffractor are derived from the extinctions noted in a pattern. Helical diffractors yield only a limited number of reflections, and the analysis may be based on the presence of diffraction maxima predicted from the selection rules, as well as absence of reflections in forbidden regions of reciprocal space.

It should be kept in mind that this kind of treatment is based on the analysis of the transforms of individual helical distributions. Any packing arrangements affect the transform by extinctions, and thus complicate the task of elucidating the helical configuration. Thus, it is desirable to eliminate all lattice experimentally so that unsampled intensities appear on the x-ray diagram. Certain packing difficulties are discussed more fully in Appendix I .

The following section shows how the basic aspects of the structure may be derived from the position of the maxima in a pattern. Some geometrical concepts useful in the interpretation of helical patterns are first developed.

(1) Helix Geometry**

All the points on a helix fall on a cylindrical surface. If this surface is split in a direction parallel to the axis, and laid flat, an array of parallel lines is obtained. This corresponds to the mapping $\phi = kX'$ (see Figure 11a). Any helix with regularly distributed discontinuities along its length will then reduce to a net consisting of a number of unit cells in the $X'Y'$ plane (Figure 11).

In general, helix-nets may be classified as single-cell or multiple-cell. The single-cell helix-net is defined as that in which no node exists on the line joining O to O' . The multiple-cell helix-net has more than one unit cell in the X' direction so that one or more nodes exist on the line joining O to let us say O'' in Figure 11b.

Within the single-cell helix-net various families** of helices whose members include all the nodes may be constructed (dashed lines in Figure 11a). These are related by screw axes coincident with the helix axis. We define the primitive helix as that which includes all the nodes in the cell. It is generated by joining an origin (O or O' in Figure 11a) of the cell with the lowest node in the cell ('a' in Figure 11a). In the single-cell helix-net there will be two primitive helices of opposite sense of twist, and the sum of the number of turns in each primitive helix is equal to the number of nodes in the cell. The genetic helix is the primitive helix with fewer number of turns.

No primitive helices exist for the multiple-cell helix-net.

It is obvious that the smallest family of helices which includes all

* Useful references: Bravais, L., and Bravais, A. (1831); Tate, G.P., (1872); Thompson, D.W. (1942).

** All the members of a particular family of helices have the same radius and pitch.

the nodes on this compound net is one in which the number of strands is equal to the number of unit cells in the cable. Further, the members of this family of helices are related by a rotation axis coincident with the helix axis.

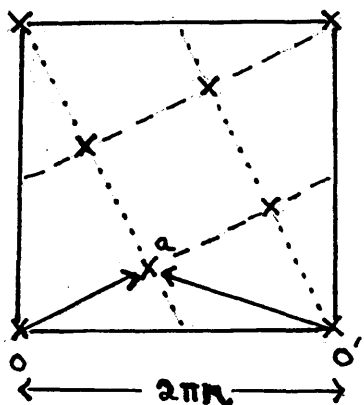


Figure 11a

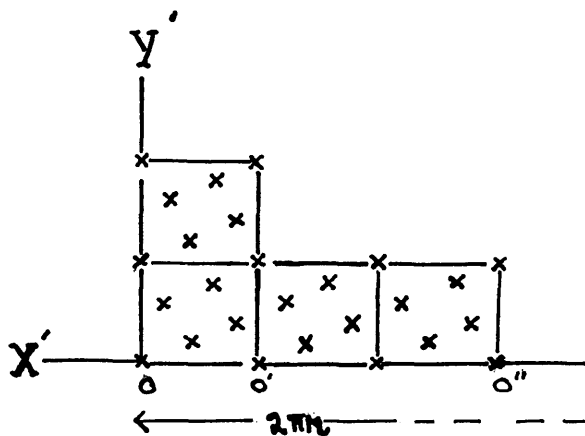


Figure 11b

(2) Interpretation of the pattern

From a consideration of the selection rules and the transforms in connection with the helix geometry we may deduce certain general features useful in interpreting helical patterns.

(a) Meridional reflections correspond either to the discontinuities in the helix, or to the period of the minor coil in the coiled-coil.

This is apparent from equations (3) and (5). Inspection of their transforms shows that for the case when $\lambda = N_1$ or M respectively, meridional reflections are predicted.

(b) Near-meridional reflections correspond to specific helical aspects of structure. Two cases may be considered.

1. The discontinuous helix will have diffractions of greatest strength and closeness to the meridian on layer lines whose indices are $\lambda = N_0, (M+N_0)$, since the transforms for these cases have J_1 Bessel function terms. It may be noted that the indices N_0 and $M-N_0$ are equal

to the number of turns in each of the primitive helices in the structure's net cell. This corresponds, of course, to these turns being equivalent to the planes of highest scattering power in the structure. Further, the symmetry about M results from each meridional reflection acting like a displaced origin.

Since the N_0 and $(M \pm N_0)$ layer lines will be strong and near-meridional, and since the layer line where $\lambda = M$ will be meridional, a pattern may be examined to see whether the relationships

$$N_0 + (M - N_0) = M \tag{7a}$$

and

$$(M + N_0) - N_0 = M \tag{7b}$$

are obeyed by the appropriate reflections. If this is true, the pattern may be characterized in terms of a discontinuous helix and its net immediately deduced.

2. The continuous coiled-coil will have near-meridional strong reflections on layer lines where $\lambda = N_0, (N_1 \pm N_0)$, since the transforms will consist of the product of one J_1 Bessel function and three J_0 's (assuming the value of the J_s Bessel function factor is appreciable).

We may then write down

$$N_0 + (N_1 - N_0) = N_1 \tag{8a}$$

$$(N_0 + N_1) - N_0 = N_1 \tag{8b}$$

From (7) and (8) the correspondence between N_1 and M is clear and a net which is based on (7) might equally well describe (8).*

 * The discontinuous coiled-coil will reduce the sum of two nets if the period of the discontinuities is different from the period of the minor coil, $(M \neq N_1)$. This compound net will consist of one primitive helix of N turns and two primitive helices with $(aN - N)$ and $(bN_1 - N)$ turns respectively, where a and b are integers. N is the smallest number of turns which accommodates an integral number of nodes corresponding to aM and bN_1 . Equations (7) and (8), together, describe this situation.

(c) The period of a helix

If P/p can be expressed as the exact ratio of whole numbers, i.e., $P/p = M/N_0$, then there is an exact period to the structure, $G = N_0 P = Mp$. This exact repeat may be quite large and often there will be combinations of smaller integers which approximate the correct ratio:

$$P/p = M/N_0 \approx (M - a)/(N_0 - b)$$

If this approximation satisfies the x-ray diagram within a certain error, it is often more feasible to work with the smaller period. (For a discussion of this problem see Cochran, Crick, and Vand, 1952).

(3) Ambiguities in the analysis

(a) Net ambiguities

1. Net-helix ambiguity:

The most profound ambiguity in this analysis is that of the net versus the helix as the actual diffracting structure. It can be shown (Crick, 1953) that the Fourier transforms of the net (with rotation) and the helix place intensity at similar loci in reciprocal space. The net and the helix have, therefore, a formal equivalence.

If much lattice is present in the diffracting system, the diffraction line shapes cannot be determined. It should be noted, however, that the transform of a helix gives little intensity after the first few maxima, even in the presence of a well-developed lattice. On the other hand, numerous row lines would indicate a net of large extent.

In some cases it may be possible to eliminate most lattice. Differences in the shapes and 'areas' of the diffraction maxima are then expected for the two kinds of structure. The rotation diagram of a net

derives from the intersection of reciprocal rods rotated into the sphere of reflection. The transform of a helix is determined by Bessel function maxima.

In addition, other non-crystallographic information may be brought to bear in determining which of the two kinds of structure is correct. Stereochemical requirements and analysis of the system by electron microscopy, ultracentrifuge, and other physical-chemical techniques may yield information which favors one of the two possibilities.

2. The single-cell versus the multiple-cell ambiguity:

This ambiguity is discussed fully in Appendix I. It is shown there that the transform of ^a cable consisting of A discontinuous helices, related by an A-fold rotation axis, has the following selection rule:

$$A (N_0/A)q = \ell + Mm'$$

where $n = Aq$ for each ℓ .

This means that the Bessel functions in the Fourier transform of a helix are multiples of the number of cells determining the width of the helix-net. Thus, in indexing a diffraction diagram, the assignment of a J_1 Bessel function to the prominent near-meridional reflections corresponds to the assumption of a single-cell helix-net. Similarly, the assignment of higher order Bessel functions to these reflections implies multiple-cell helix-nets.

Limits may be imposed on the number of cells wide a particular helix-net may be. The higher the order of the Bessel function assigned, the larger must be the radius of the diffracting unit to account for

the position of a particular maximum on the x-ray diagram. When the radii become too large to meet other requirements, for example, of density or of packing, the associated helix-nets and any wider ones, need not be considered.

(b) Connection ambiguities

The preceding analysis has been based on a treatment of idealized diffracting systems where periodic discontinuities are reduced to 'nodes'. In order to use the Fourier transforms developed, these nodes were treated as point scatterers. It is clear, however, that in the actual structure, the nodes correspond to any periodic variations of electron density which occur along the scattering backbone. Thus, for a protein, a node might correspond to a group of amino acid residues in which one residue has a smaller side chain than the others, or to the minor coil in the continuous coiled-coil. Included by the node might be more than one polypeptide chain, and different nodes might belong to different chains related by various screw axes (see Figure 11a). Thus, by designating the 'net' of a helix, the helical analogue of the crystallographic lattice has been specified by the node arrangement. However, the chemical connection about the node remains to be specified. Stereochemical arguments, complete structure factors, and other considerations must be used in distinguishing among the many possibilities. Appendix I gives some general examples of the problem and this ambiguity is discussed at length with specific reference to collagen in a later section of this thesis.

2. Application of helical diffraction theory to collagen

a. The basic helix-net of collagen

The appearance of the collagen pattern immediately suggests a discontinuous helical diffractor. The presence of two strong near-meridional reflections, each displaced from a true meridional reflection by the same amount, is a striking feature. Thus, we note the relation:

$$3 + 7 = 10 \text{ (for indices assigned on the basis of a 28.6 \AA. period.)}$$

The correct helix-net may be described as ten discontinuities in three turns of the genetic helix. This is shown in Figure 12. The basic screw corresponding to the genetic helix, is a translation of 2.86 - 3.1 \AA./node, and a rotation of 108° /node. Indexing on the basis of a 20 \AA. pseudo-period (Cohen and Bear, 1953) yields a very similar net with seven nodes in two turns.

We may note that the three-chain model for the collagen protofibril suggested by Pauling and Corey (1951) has nine discontinuities in one turn, and the γ helix model (Bear, 1952) has seven discontinuities in four turns. These do not give the correct distribution of diffracted intensity for the collagen diagram (Pauling and Corey, 1953; Cohen and Bear, 1953).

Starting with the correct helix-net, and using the selection rule for the discontinuous helix (equation 5) we can draw up a table which gives the orders of the Bessel functions expected for each layer line in the 28.6 \AA. period. This is shown in Table 4. If one compares

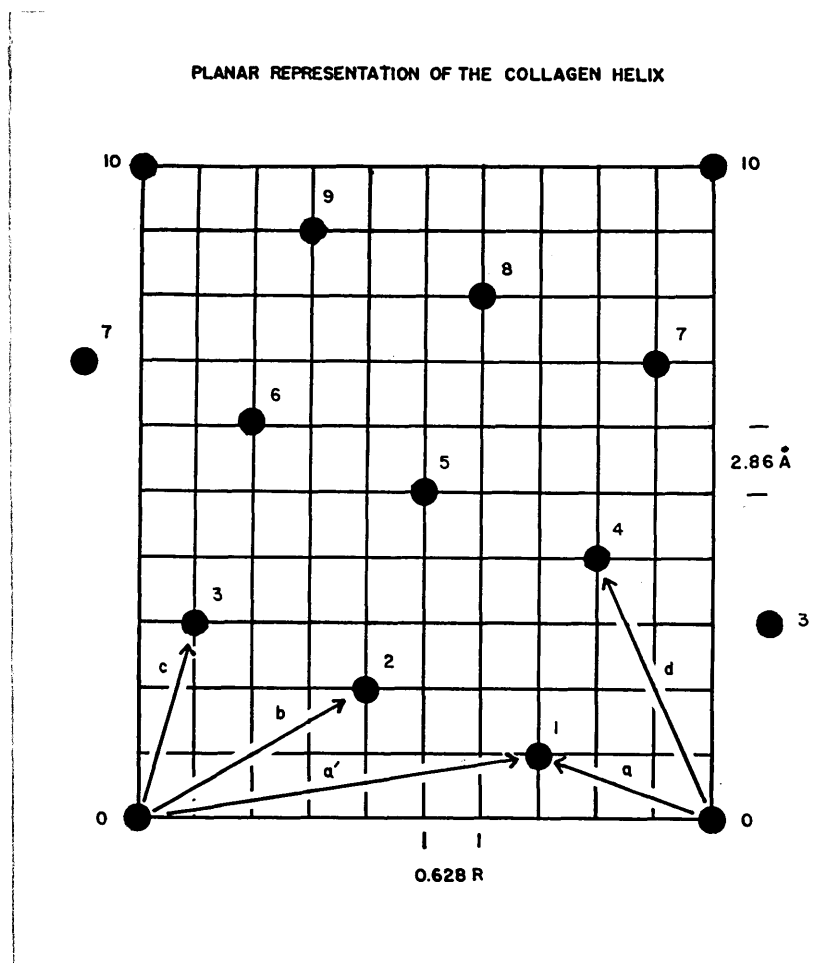


Figure 12

Table 4

Bessel Function Orders for Discontinuous Helix for Collagen

$$n = \frac{\lambda - 10 m'}{3}$$

n = Bessel function order
 λ = Layer line index
 m' = Any integer

d = c^*/λ , A.	λ	m'						
		$\bar{3}$	$\bar{2}$	$\bar{1}$	0	1	2	3
∞	0	10	--	--	0	--	--	10
28.6	1	--	7	--	--	$\bar{3}$	--	--
14.3	2	--	--	4	--	--	$\bar{6}$	--
9.56	3	11	--	--	1	--	--	$\bar{9}$
7.15	4	--	8	--	--	$\bar{2}$	--	--
5.72	5	--	--	5	--	--	$\bar{5}$	--
4.77	6	12	--	--	2	--	--	8
4.09	7	--	9	--	--	$\bar{1}$	--	--
3.58	8	--	--	6	--	--	$\bar{4}$	--
3.18	9	13	--	--	3	--	--	7
2.86	10	--	10	--	--	0	--	--
2.60	11	--	--	7	--	--	$\bar{3}$	--
2.38	12	14	--	--	4	--	--	$\bar{6}$
2.20	13	--	11	--	--	1	--	--
2.04	14	--	--	8	--	--	$\bar{2}$	--
1.91	15	15	--	--	5	--	--	$\bar{5}$
1.79	16	--	12	--	--	2	--	--
1.68	17	--	--	9	--	--	$\bar{1}$	--
1.59	18	16	--	--	6	--	--	$\bar{4}$
1.51	19	--	13	--	--	3	--	--
1.43	20	--	--	10	--	--	0	--

* Assuming a 28.6 A. period.

the predicted diffractions with the observed ones, excellent agreement is found. Thus, in Table 4 the lowest Bessel function predicted for each observed layer line is noted. However, for spacings greater than the 2.86 A., the faintness, arcing and diffuseness of the reflections are such that the indexing is not reliable and too much stress should not be laid on these reflections. In addition, the atomic scattering factors will have effects in this region which are not taken into account by the simple point discontinuity model used in this preliminary analysis. Some notion of the intensity distribution is gained by plotting the position of the lowest order of Bessel function predicted for each layer line on some reasonable radial scale. This is shown in Figure 13 for the first 10 layer lines of a discontinuous helix with radius 3 A. As a first approximation, one may consider that the lower the order of the Bessel function, the greater the intensity. For true intensity calculations, of course, various damping factors which are functions of position in reciprocal space must be taken into account.

As an aid in evaluating models, an 'optical transformer' was designed and constructed by Mr. Harold Wyckoff. Appendix II gives a description of the system and the particular methods used in obtaining the diffraction patterns. We may note that for helical diffractors whose transform amplitudes have cylindrical symmetry, such an apparatus is particularly useful, since any one section through the origin of reciprocal space (corresponding to a projection in real space) gives the complete intensity distribution. Figure 14 shows the projection of the basic discontinuous helix for collagen, and the optical diffraction pattern obtained. The relative positions of the chief maxima are as anticipated from Figure 13.

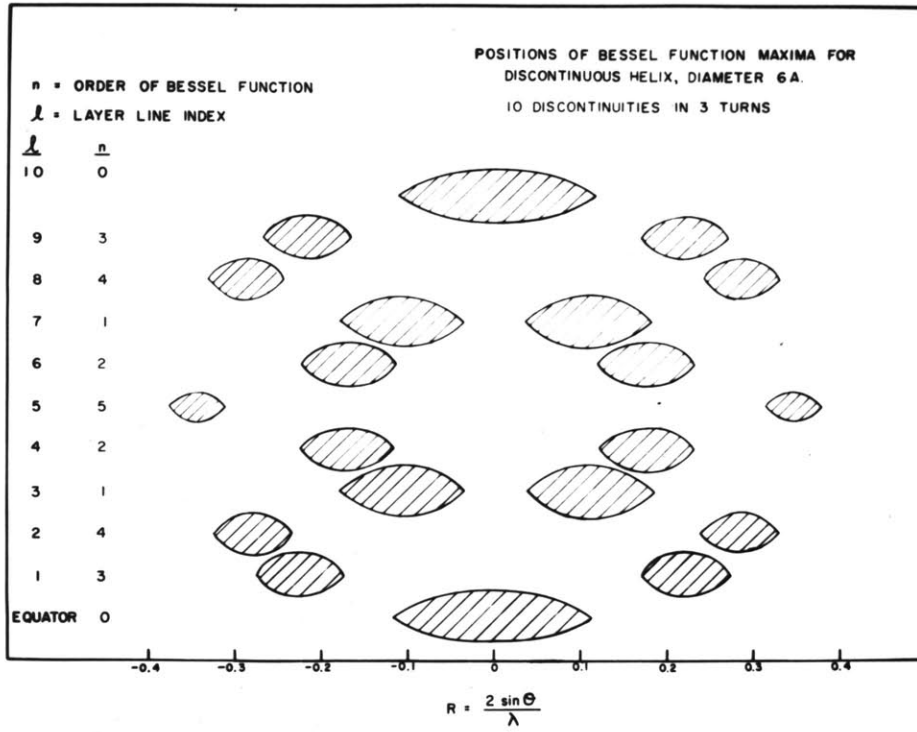


Figure 13

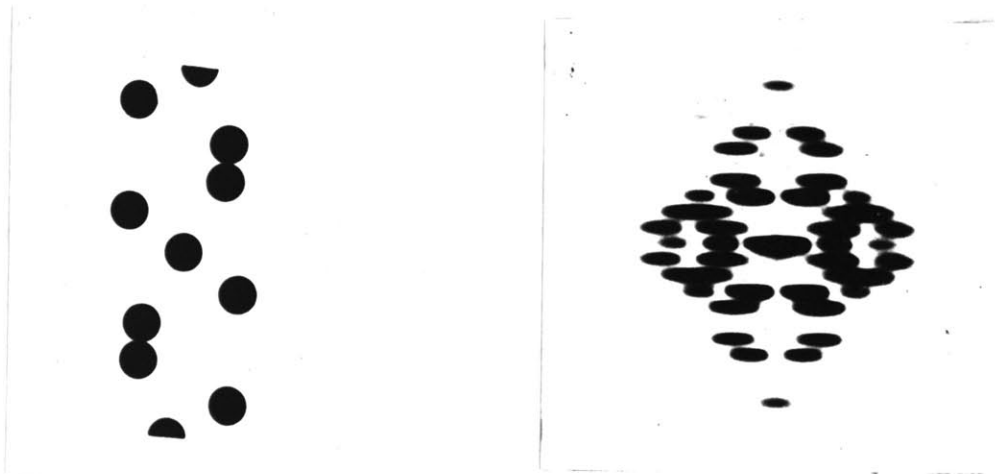


Figure 14a

Figure 14b

Projection and optical diffraction pattern of genetic helix for collagen

A comparison of this optical diffraction pattern with the x-ray diagram obtained with moistened KTT (Figure 6) shows an essential similarity in the two patterns. In particular, the strength and position of the third, seventh, and tenth layer lines should be noted, as well as the presence of the heart-shaped equatorial maximum corresponding to the 4.5 Å. equatorial intensity. The chief discrepancy is the prediction of relatively strong fourth and sixth layer lines, which do not appear (with the possible exception of the fourth) on the wide-angle diagram.

It should also be pointed out that the helix-net which was derived for the collagen protofibril was based on the analysis of the sharp near-meridional diffractions. The fact that the intense heart-shaped equatorial maximum at 4.5 Å. appears in transforms of this basic net is of interest. However, the presence of diffuse intensity maxima in other regions of the wide-angle pattern has been mentioned before (see Figure 6). Whether these will be explained by the same structure which accounts for the meridional reflections remains to be seen.

b. The structural interpretation of the collagen helix-net

The basic helix-net represents those parts of the protofibril which diffract coherently. In the preceding section, it was shown that very good agreement is found between observed diffraction maxima, and those predicted by a discontinuous helix. However, all the ambiguities discussed above are present in this analysis and must be considered.

(1) Helix versus net ambiguities

The primary ambiguity is the helix versus the net as the actual diffracting unit. Without a complete analysis of the shape of the diffraction maxima, one cannot conclusively prove that the x-ray pattern is not derived from a net rotation diagram. However, all the evidence is

consistent with the assumption of a cylindrical diffracting unit for the protofibril. Thus, the shape of the layer line maxima on patterns from moistened specimens (showing little lattice) have characteristics of Bessel functions (Figure 6). In particular, the first minimum and second maximum on the equator can both be accounted for by a hollow cylindrical diffractor of radius 5.7 Å. (the Fourier transform is then a J_0 Bessel function). The pattern from dry tendon, showing sampling by a poorly developed lattice, is consistent with the assumption of hexagonal packing of cylindrical units. In addition, electron microscopy of the fibril indicates a uni-axial structure. Once the cylindrical nature of the individual diffracting unit is assumed, the wide-angle diagram can be interpreted on the basis of a discontinuous helix, and as shown above, the agreement with observed intensities is very good.

It is highly probable, therefore, in the case of collagen, that the net is only a formal and not an actual solution of the diffraction problem.

(2) Restrictions on the helix

The next stage in the analysis, where the number of nodes in the helix and the chemical connections about the nodes are described, is far more difficult. In order to make a solution feasible, all possible restrictions on the model, from chemical, stereochemical and physical data (including the x-ray diagram) must be considered.

(a) Number of residues per node

The density of collagen is usually taken as 1.35 (Astbury, 1940). This is the value one obtains for dry collagen by flotation in mixtures of organic solvents (Rougvie and Bear, 1953). However,

Pomeroy and Mitton (1951) have pointed out the errors involved in the use of such a method, and by displacement of nitrogen gas, they determined a 'real density' of 1.41 for dry-calf hide collagen.

In order to calculate the number of residues which must be placed at each node for the single-cell helix-net we may proceed with an argument like that given by Bear (1952). We assume that the protofibrils in collagen can be considered as hexagonally packed cylinders. The distance between planes is then 10.6 A., the value of the equatorial spacing for the driest specimens. Therefore, the distance between centers of the cylinders is $10.6 \text{ A.} / \cos 30^\circ$, or 12.24 A. This gives a value of 130 A^2 for the cross sectional area of each protofibril. The cylindrical volume for each node in a 28.6 A. period is then 372 A^3 . If the density is taken as 1.41, it contains a weight of about 315.

The serious difficulty now confronts us as to what residue weight one should use. Bear (1952) has given reasons for believing that the collagen wide-angle diagram is derived mostly from the interband or well-ordered region of the fibril. The relative extent of this region is not known. Further, he has given convincing arguments for the localization in the interbands of residues with hydroxylic rather than acidic or basic side chains. He pictures the non-polar side chains (which make up about 65% of the residues) as being distributed among both the bands and interbands.

If it is assumed that there is no difference between band and interband, the average residue weight of 93 for all amino acids there present, permits about 3.5 residues per node. If, however, the assumption is made that only non-polar and hydroxylic residues are in

the interbands, their average residue weight makes possible as many as four residues per node.

Thus, in building models we are faced with the problem of whether to place 3, 3.5, or 4 residues about each node of a single net cell. This argument depends on the assumption of relatively small differences between band and interband. If greater differences occurred, the numbers of residues per node might be quite different in the two regions.

(b) The lattice ambiguity: Number of nodes per discontinuity

The next problem to deal with is how many net cells wide the collagen helix may be. The answer to this depends partly on the answer to (a). Two kinds of argument may be used.

The maximum extended length of an amide residue is 3.64 Å. (Corey and Donohue, 1950). Further, it is impossible to have a non-integral number of residues compose each node.* Using these facts, it is clear that the collagen helix cannot comprise more than four net cells. In this case only one residue is associated with each node, and it is impossible to have fewer than one per node.

Moreover, for models built from only one kind of net, only helix-nets one or two net cells wide need be considered. This is so since the assumption that the third layer line maximum is a J_3 or J_4 Bessel function requires the radii of the corresponding cables to be larger than the 6 Å. limit imposed by the dry pattern.

* The only exception to this is the case of the coiled-coil (see Appendix III). But since the coiled-coil comprises only one net cell in width, it is not relevant to this ambiguity.

Helices composed of combinations of single- and multiple-cell nets have transforms whose maxima depend on all the nets involved. In this case, a net three or more cells wide might be permitted.

(c) Stereochemical restrictions

In making the chemical connections, certain rules are to be followed. Pauling and Corey have formulated the general plan of attack for the synthetic approach to protein structure (see Corey and Pauling, 1953 and Pauling and Corey, 1953, for references). Donohue (1953) has recently reviewed the criteria used.

The structures are built of planar amide units in which the *trans* configuration seems more probable than the *cis*. The maximum number of hydrogen bonds are to be established, and these bonds have prescribed lengths, and angular limits between the N-H / ^{and} O-N vectors. For the particular case of collagen, Ambrose and Elliott (1951) have presented evidence from infra-red dichroism that the hydrogen bonds are generally oriented in a direction perpendicular to the fiber axis.

It is clear that these stereochemical restrictions place very great limitations on the number of models which may be constructed on any given plan. However, in the development of these rules, side chain effects were not considered, and it seems likely that some variation from these stereochemical requirements may be tolerated in particular situations.

(d) The imino residues in collagen

Collagen has an amino acid composition which is distinctly different from that in all other proteins. This is due to the extraordinarily high content of proline and hydroxyproline. From the data

of Bowes and Kenten (1948), Bowes, Elliott and Moss (1953) and Brown, Kelly, and Watson (1953) for mammalian collagen, these amino acids occur in almost equal amounts and they make up, on the average, at least one out of every five residues.

Moreover, these imino residues present special stereochemical problems, in addition to the lack of a hydrogen bonding locus on the nitrogen. The large pyrrole ring must be accommodated by the structure in which the proline is placed, and there is a loss of rotational freedom about the N-C α bond of the residue. These conditions make it impossible to accommodate proline in one of the two possible senses of twist for the α helix (Pauling, 1953). At present not enough evidence is available to decide whether the trans configuration is more probable than the cis or even whether the planarity of the peptide bond is maintained for these residues.

(e) Extensibility

Electron microscope evidence of Schmitt, Hall and Jakus (1942) showed that fibrils stretched to several times their length still maintained their pattern of bands. This might be interpreted to mean that the protofibrils in collagen are extensible up to two and a half times the normal length (Bear, 1952). However, explanations of the extension are possible which do not necessitate uncoiling in the part of the protofibril which gives rise to the wide-angle pattern. Therefore, in view of the very severe and possibly artificial limitation such a restriction places on a model, it is probably unwise at this time to use this as a structural criterion.

(3) Models for collagen

The collagen model problem has presented unexpected difficulties. Since the basic net is known, it might be expected that at least several models would fulfill the necessary criteria, and that these would have to be evaluated with regard to details of the wide-angle pattern. However, although in theory there are very many different arrangements of residues which satisfy the node pattern, the stereochemical and chemical restrictions are such that very few models look promising. Cowan et al. (1953) have listed several of the general types which might be possible, but no detailed model was suggested.

In fact, since the basic net was determined last year, only one model has been proposed which fulfills to any reasonable degree the necessary requirements. This is the model proposed by Crick (1954). It is a two-strand cable, based on the two-cell helix-net of collagen. Each strand has $3/2$ turn in 29.5 Å. The infra-red dichroism of collagen is accounted for by having hydrogen bonding perpendicular to the axis of the helix. However, the stereochemical requirements are not completely satisfied since there is a crowding of atoms in violation of van der Waal's radii. In addition, it is an all cis peptide bond structure. The optical transform, made for this model by Mrs. Chow, shows that the agreement with the collagen wide-angle diagram is good (see Figure 15). One expects that any model built on the net plan will give the three, seven, and ten reflections, but it is the relative intensities and positions of these reflections which must be accounted for. Further evaluation of this model is being carried out by Mrs. Chow.

It appears at this time, therefore, that no entirely satisfactory model has been proposed for the collagen protofibril.

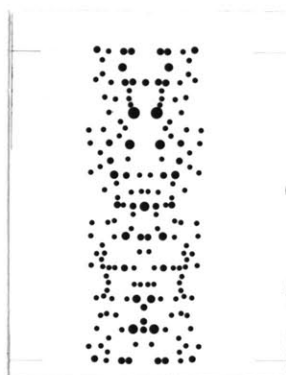


Figure 15a

Projected model of Crick (1954)
two strand cable for collagen
(includes β , γ , and δ carbon atoms)

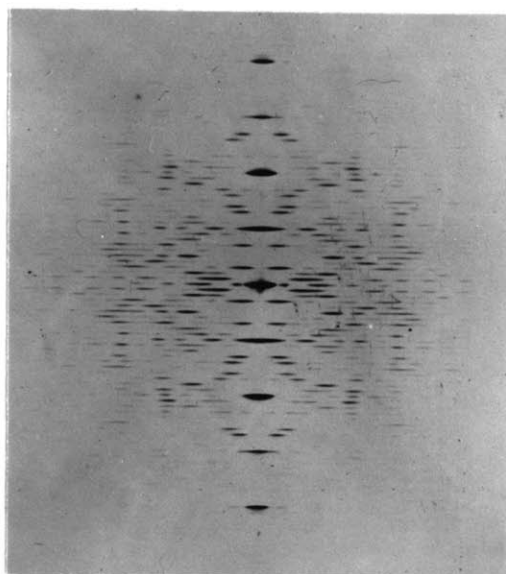


Figure 15b

Optical diffraction pattern from
Figure 15a

Figures 15a and b were supplied by Mrs. J. Chow.

C. Conclusions

1. The wide-angle x-ray diagram of unstretched collagen can be indexed by a 28.6 Å meridional period. Periods up to about 30 Å. were obtained by high tension.

2. The diagram is that of a helical diffractor. The genetic helical arrangement is ten nodes in three turns. The basic screw, therefore, has a translation of about 3 Å., and a rotation of 108° .

3. Helical diffraction ambiguities are encountered in the more detailed analysis of the pattern.

4. Thus far, no model has been proposed which fulfills all the necessary physical and chemical criteria.

Chapter III

Optical Rotation Studies

Two important relationships describe the optical rotativity of a substance. The first expresses the value of the rotation independently of the concentration at a particular wavelength and temperature. The other indicates the dependence of the rotation on the wavelength of the light used in the measurements.

Thus, we have the following definitions:

The specific optical rotation of a solution of an optically active substance is defined as:

$$[\alpha]_{\lambda}^T = \frac{\alpha}{c \ell} \cdot 100$$

where α is the observed rotation in angular degrees at temperature T and wavelength λ ; c is the concentration of the substance in grams per 100 cc. of solution; and ℓ is the length of the tube in decimeters.

Drude (1900) formulated the relation for the wavelength dependence of rotation. This may be expressed as:

$$[\alpha]_{\lambda}^T = \sum \frac{k_m}{\lambda^2 - \lambda_m^2}$$

where k_m are the rotation constants; λ_m^2 are the dispersion constants; and are, in principle, the absorption bands controlling the dispersion. The formula is not valid within and close to an absorption band.

Classification of the kinds of rotatory dispersion which may be found have been made by Lowry and Dickson (1913), Lowry and Owen (1930) and Lowry (1935). If a one-term Drude equation is followed,

$$[\alpha]_{\lambda}^T = \frac{k}{\lambda^2 - \lambda_0^2} \cdot$$

This is called simple dispersion.

If more terms are necessary, the substance is said to show complex dispersion.

If $1/[\alpha]$ is plotted against λ^2 , and a straight line is obtained, the substance shows simple dispersion. The slope of the line gives the rotation constant k , and the intercept gives the dispersion constant λ_0^2 .

Dispersion measurements are important for several reasons. If a quantitative comparison of the optical activity of different substances is to be made, the dispersion constants should relate to the same wavelength region in order that the comparison be justified. Thus, if different absorption bands were controlling the rotation of two different compounds, this would be clear from the dispersion curves and comparison of the rotation values could not be made. Furthermore, any theoretical relation between molecular structure and chemical composition is based upon the dispersion characteristics of the material and not simply upon the rotation at one wavelength (cf., Discussions of the Faraday Society, 26, 1930). In a problem as difficult as the relation between optical rotation and molecular structure in proteins, all information about the rotation characteristics, including the rotation and dispersion constants, should be determined.

A. Experimental data

1. The conversion of 'procollagen' to 'parent gelatin'

The optical rotation of solutions of ichthyocol and calf hide 'procollagen' and 'parent gelatin' was investigated. The material was prepared by a citrate extraction and the protein concentrations deter-

mined by a Biuret reagent technique. A complete description of preparative procedures and concentration determination is given by Gallop (1953).

Optical rotation measurements were made with a Schmidt and Haensch polarimeter which could be read to 0.05° . Unfiltered radiation from an Osram sodium lamp (SL/D 1-3) was used in the initial experiments and later experiments were performed using a G.E. Na 1 lamp. Temperature regulation was maintained by means of circulating water from a thermoregulated bath through metal jacketed 2 dm. polarimeter tubes. Temperature was controlled to about $\pm 1^\circ$ C. At least ten observations were averaged for each recorded reading.

Results: Figure 16 presents a typical curve where $[\alpha]_D$ is plotted against temperature at various times during heating and re-cooling cycle. From the data, the optical rotation of unheated ichthyocol 'procollagen' in citrate buffer pH 3.7 (0.15 M citrate) was found to be $[\alpha]_D^{10} = -350 \pm 30^\circ$. Upon heating the solution to 30° C. the rotation fell until reaching values of $[\alpha]_D^{30} = -110^\circ \pm 20^\circ$. The speed of this reaction varied; from one to more than twenty four hours were required for the completion of the reaction with different preparations and concentrations. At 40° C. the reaction proceeded very rapidly in every case, the rotation falling from $[\alpha]_D^{40} = -350^\circ$ to -110° within a half hour.

When the solutions were cooled, the rotations gradually rose and values of $[\alpha]_D^0$ up to about -280° were obtained, depending upon temperature and length of cooling. The specific rotation of -350° characteristic of the unheated 'procollagen' was not obtained, but

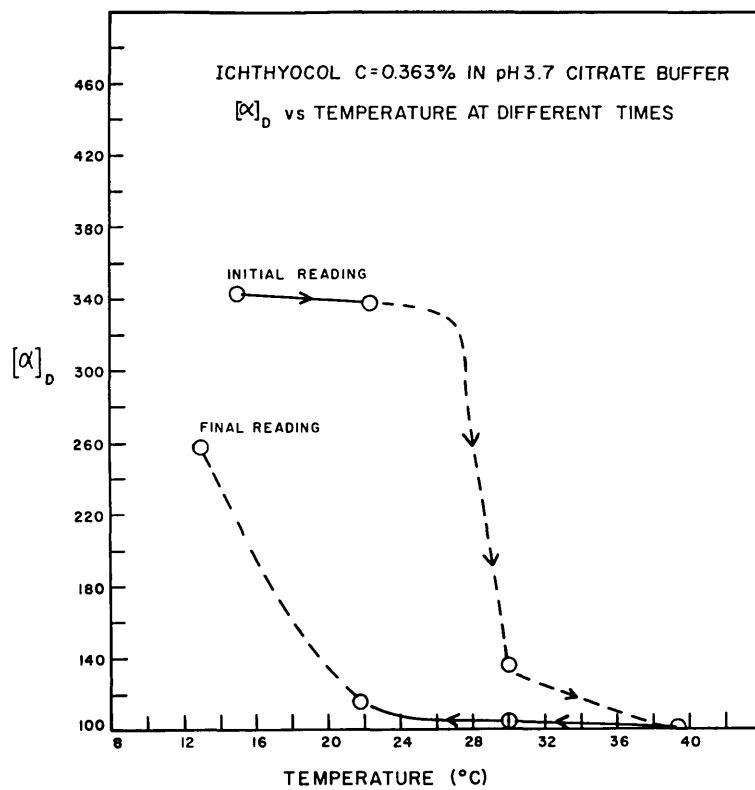


Figure 16

longer equilibration at low temperature might have produced rotations greater than -280° .

Once the value $[\alpha]_D = -110^{\circ}$ has been reached by the system, the mutarotation phenomenon is reproducible; upon cooling to a certain temperature the rotation rises to a characteristic value, and when the solutions are reheated the rotation gradually falls until, at a temperature of 30° C., the limiting value of -110° is again obtained (see Figure 16). This kind of rotativity behavior is characteristic of gelatins (Smith, 1919).

'Procollagen' preparations from calf hide showed a somewhat different temperature dependence, requiring heating to 34° C. before marked rotation changes were observable, but the values for the specific rotations (within 15%) and the mutarotation phenomenon were like those for the ichthyocol preparations.

The data presented here are consistent with those reported by Thureauux (1945) for acid extracts of various collagens. The lower rotations obtained by that author are probably accounted for by the impurity of the preparations she examined.

2. Correlation with viscosity studies

Preliminary experiments were carried out with Dr. Paul Gallop to determine the relation between specific rotation and the intrinsic viscosity of 'procollagen.' These data have been reported by Gallop (1953, 1954). For these experiments, the method used was the same as in section 1, except that two thermoregulated baths were used, one for the viscometers and the other for the polarimetry. The temperature regulation was such that the solutions in the polarimeter tubes were

maintained at about the same temperature, within 2° C., as those in the viscometers. The deviation in temperature occurred chiefly when the temperature in the two baths was changed. Two kinds of Ostwald-Fenske capillary viscometers were used which had flow times of about 60 seconds and 270 seconds for water at 20° C. No study was made of the gradient dependence of the intrinsic viscosity.

Three different runs were made. In the first, ichthyocol 'procollagen' at a concentration of 0.38% showed a slow decrease of rotation at 30° C. (incomplete in 12 hours) and a simultaneous decrease in viscosity. When the solution was heated to 39° C., both reactions went rapidly to completion (within one hour). Another run was made using a different preparation of 'procollagen' and three concentrations of protein. In this experiment the rotation reached its limiting value at 30° C. within five hours for all three concentrations, while the viscosity remained high. Figure 17 illustrates this effect for one of the concentrations.

An experiment with hide 'procollagen' gave a similar result. Figure 18 shows the specific rotation and intrinsic viscosity at different times. The intrinsic viscosity is seen to be about seven when the optical rotation has reached its limiting value. Intrinsic viscosities were determined by plotting n_{sp}/c versus c at specified temperatures and times, and extrapolating to zero concentration. Figures 19 and 20 show these viscosity data. The initial intrinsic viscosity for unheated hide 'procollagen' was found to be about 28, and that for hide 'parent gelatin' 0.4 to 0.6 at 39° C. This may be compared with values of 19 for the intrinsic viscosity of unheated ichthyocol 'procollagen' and

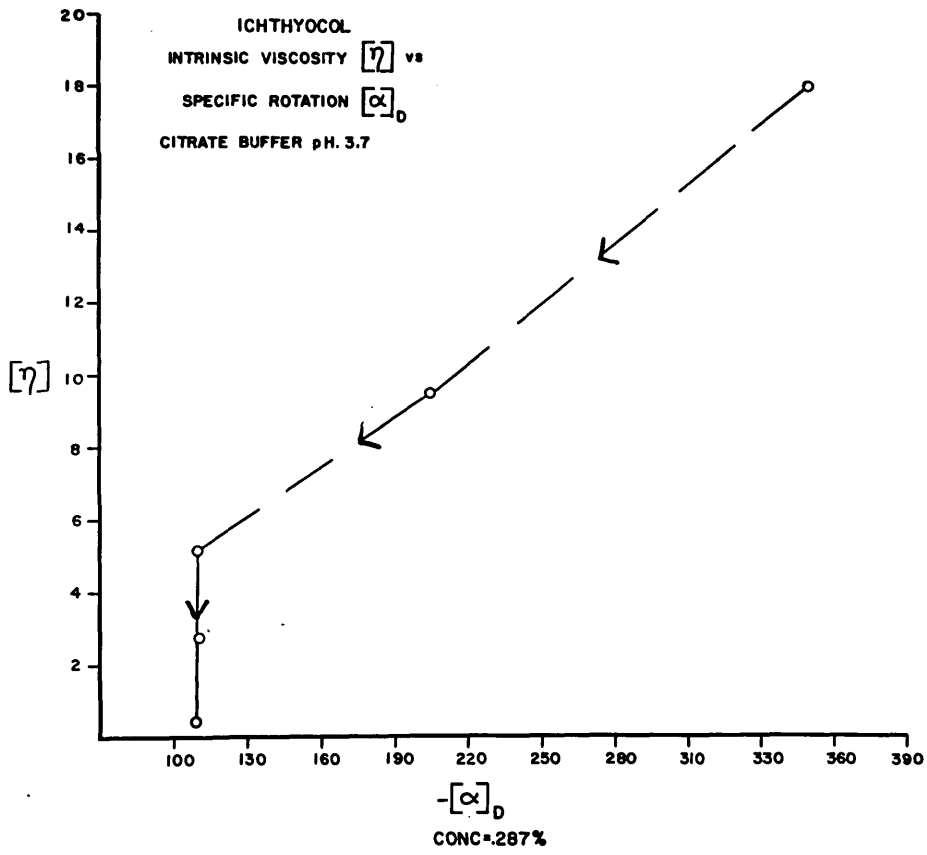


Figure 17

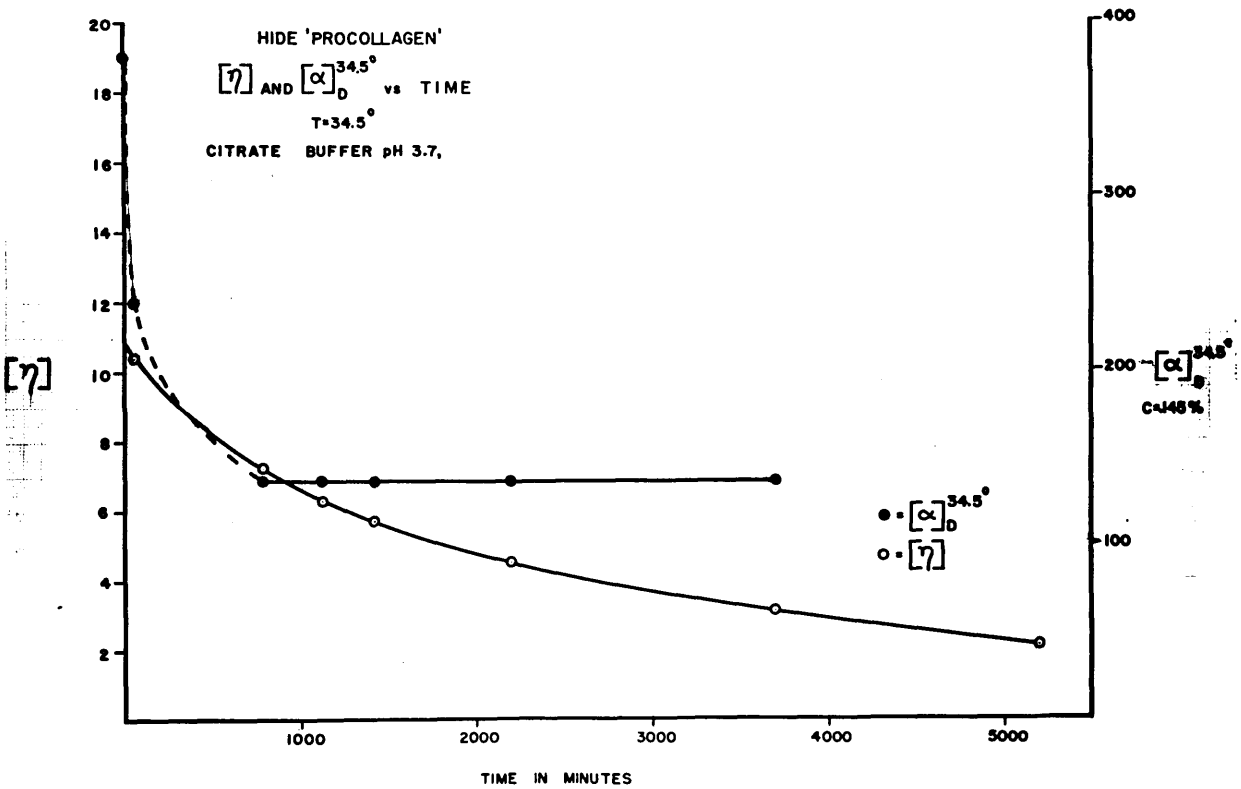


Figure 18

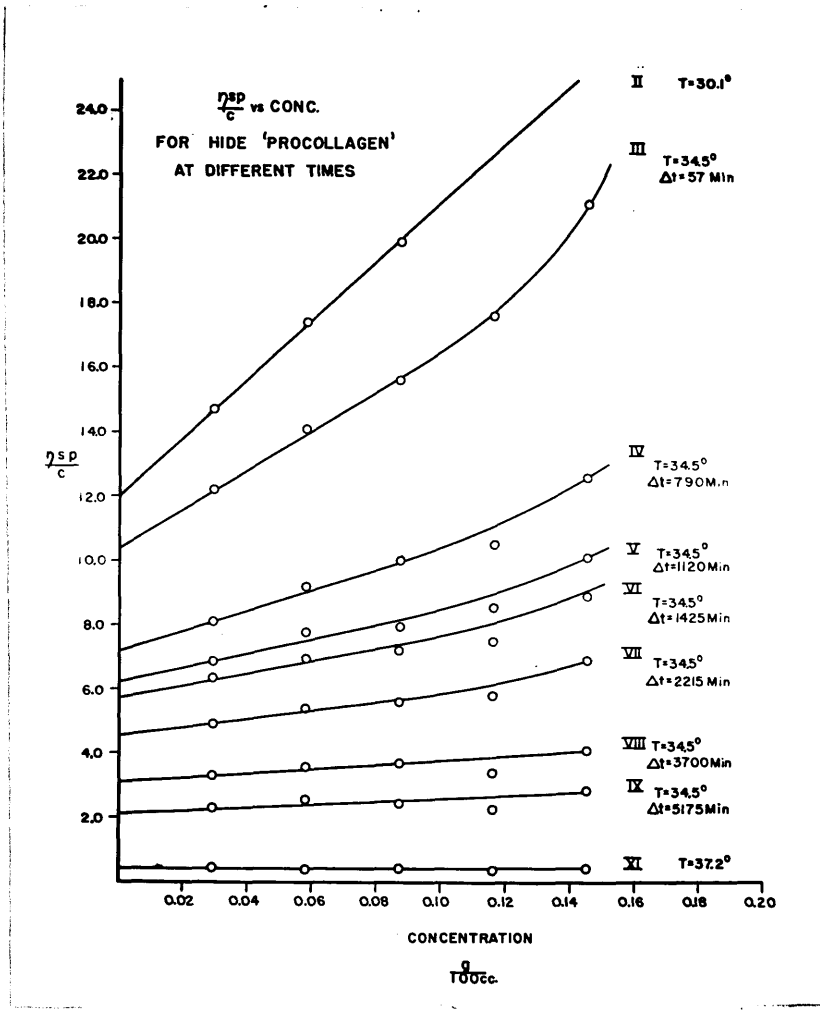


Figure 19

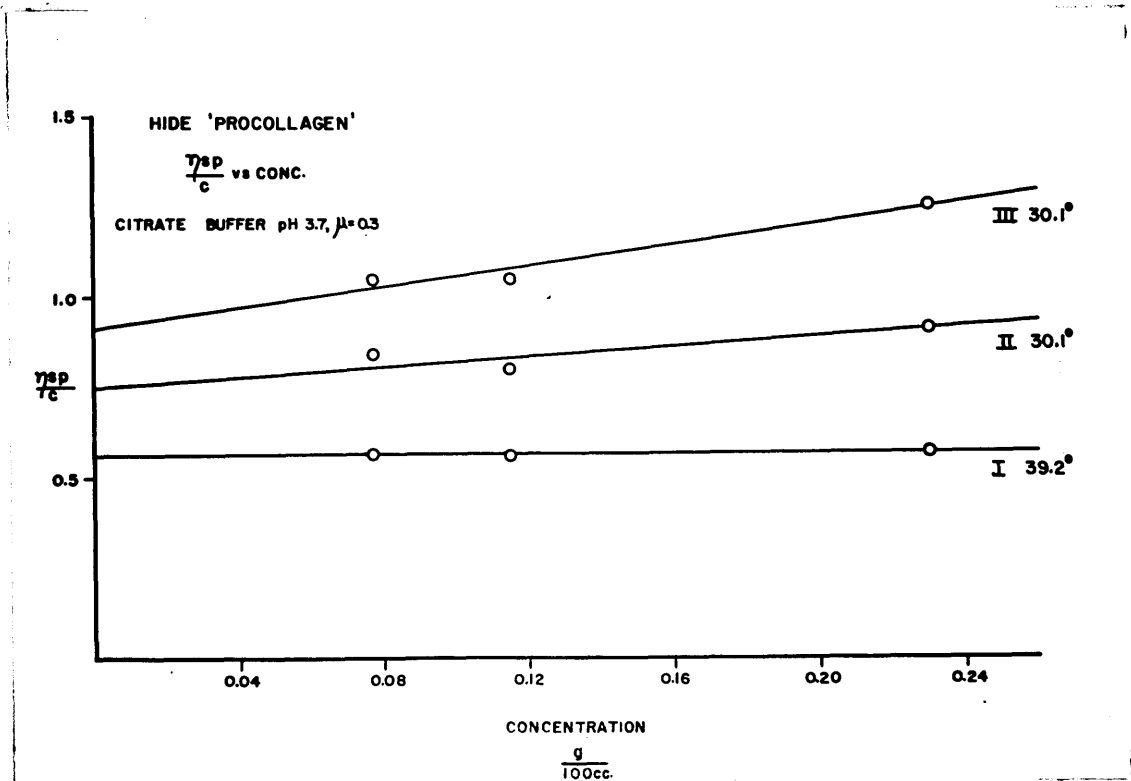


Figure 20

0.34 for ichthyocol 'parent gelatin' at 39° C.

3. Rotatory dispersion measurements

A. Rotatory dispersion measurements were carried out to analyze further the temperature effect on the specific rotation of the solutions of ichthyocol 'procollagen' and 'parent gelatin.'

Method: For these experiments a Rudolph high precision polarimeter was used. This could be read to 0.002°. In practice an accuracy of about 0.01° was obtained. Metal jacketed 4 dm. polarimeter tubes were used, and an Aminco thermoregulated bath was used for temperature control. Each temperature setting was maintained to less than $\pm 0.5^{\circ}\text{C}$. The temperature of the solutions was about 1° different from that of the circulating water, and if three tubes were run in series, the maximum temperature differential among them was about 1° C. At least ten observations were averaged for each recorded reading. The tubes were closed with rubber stoppers and aluminum foil.

Four wavelengths in the visible were used. Sources and filters are presented in Table 5 .

Table 5

$m\mu$	Source	Filter
436	G. E, H-4 Hg Arc	Corning Glass #3389 and #5113 (2.5 mm.)
546	" "	Baird Interference filter #V-1-250; Corning Glass #3-69; and Corning Glass Didymium #1-63
578	" "	Corning Glass #3480 (3.85 mm) and #502 (0.8 mm)
589	G.E. Na-1 lamp	Yellow filter supplied with Rudolph polarimeter

Concentrations of ichthyocol 'procollagen' from 0.02% to 0.46% were examined at three different temperatures. The protein preparations were stored in the refrigerator at about 4° C., then transferred to the polarimeter tubes and equilibrated for 12 hours in a water bath at 10° C. Readings were then taken. The solutions were kept overnight in the tubes at 10° C. and during the course of five hours the next day the temperature was raised to 42° C. in the bath and the tubes equilibrated at this temperature for one hour. Readings were then taken and the temperature lowered overnight. After 30 hours at 1° C. readings were again taken. This procedure was repeated for each set of three concentrations.

Results: The results of these experiments are presented in Figures 21, 22, and 23, which show the readings at $T = 11^{\circ}$, 41° , and 2° C., respectively. In order to include all of the data most clearly these are bilinear plots of $1/[\alpha]_{\lambda}^T$ vs. $\lambda^2 + 100$ c. (A 5% correction was made for each of the three lowest concentrations at 2° C. because of possible faulty sealing of the polarimeter tubes.) The following main features may be derived from the data:

(1) $1/[\alpha]_{\lambda}^T$ vs. λ^2 gives a straight line at each of the three temperatures. The intercept does not differ within experimental error for each of the three temperatures.

(2) In order to illustrate these data, rotation values from the medium concentration range were chosen. These are close to extrapolated values for unheated 'procollagen' at 11° C. and for 'parent gelatin' at 41° , and no valid extrapolation can be made for 'parent gelatin' at 2° C. Table 6 presents these values, and they are plotted as $1/[\alpha]_{\lambda}^T$ vs. λ^2 in Figure 24. Assuming a $\lambda_0^2 = 0.042 \times 10^{-8}$ cm² as the dispersion con-

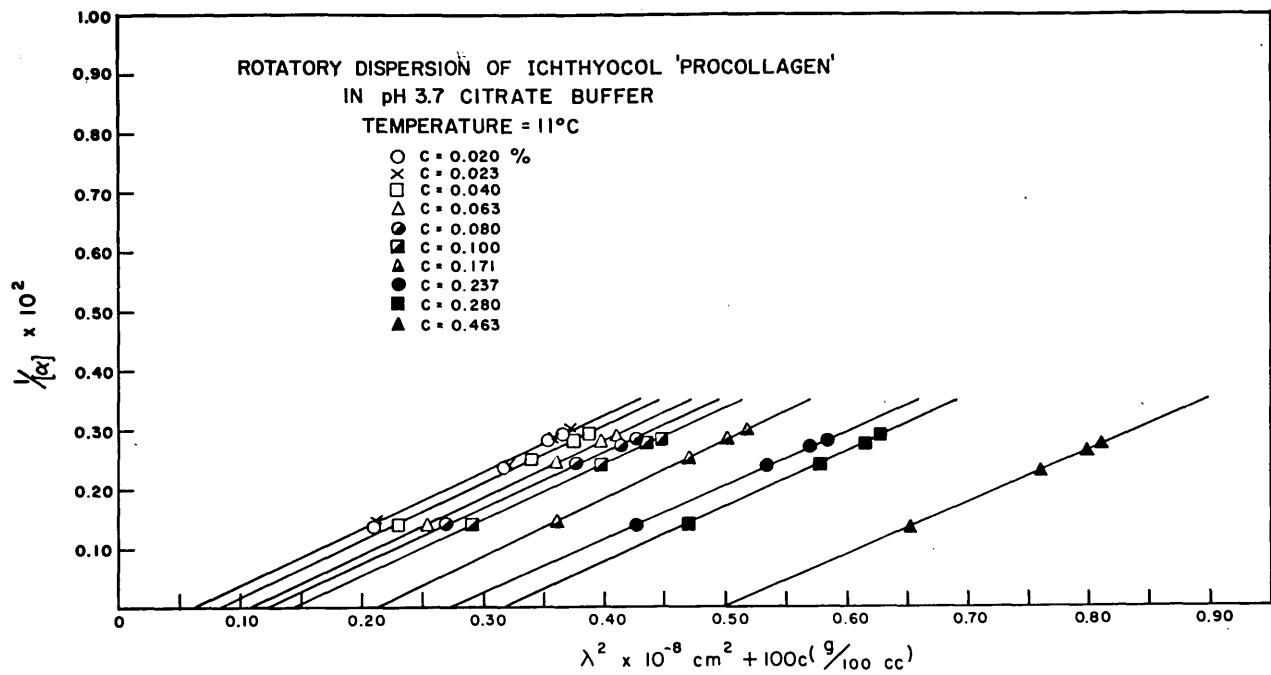


Figure 21

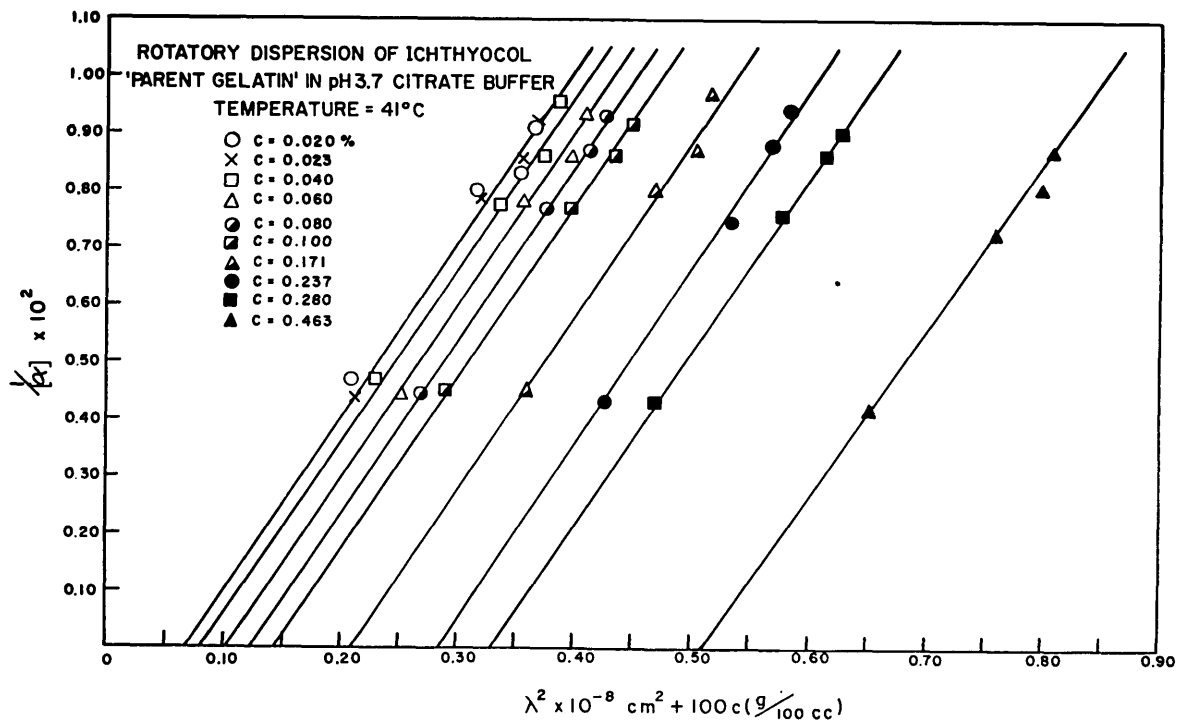


Figure 22

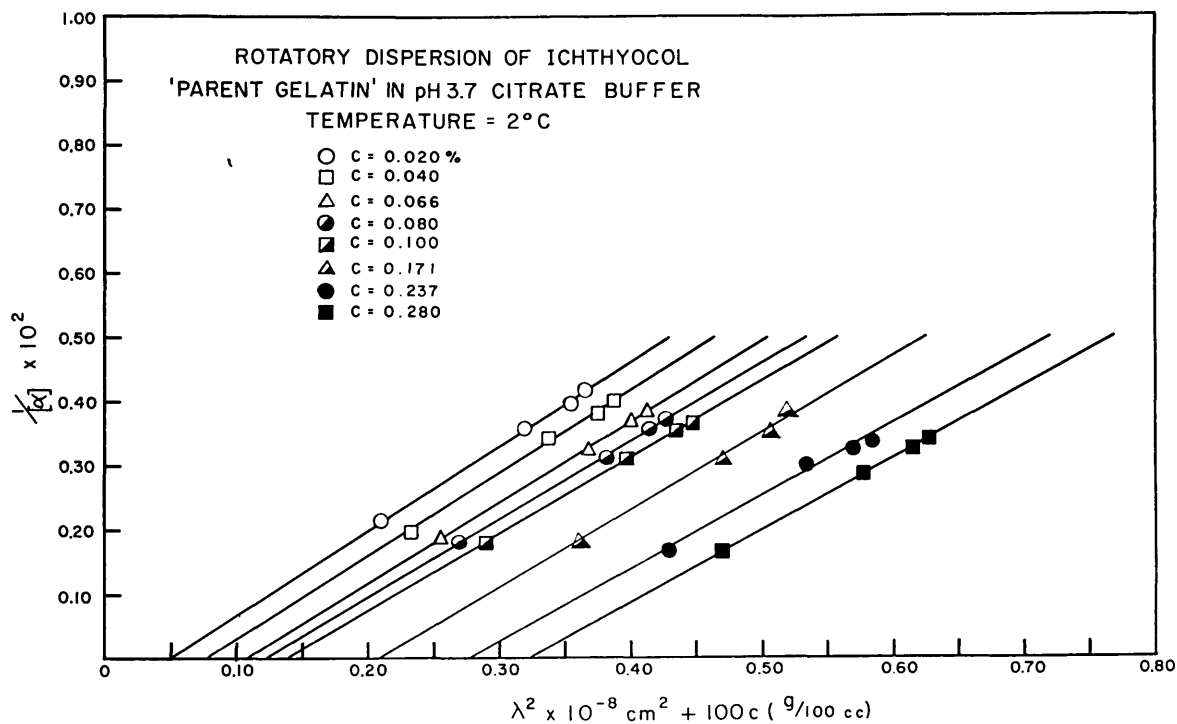


Figure 23

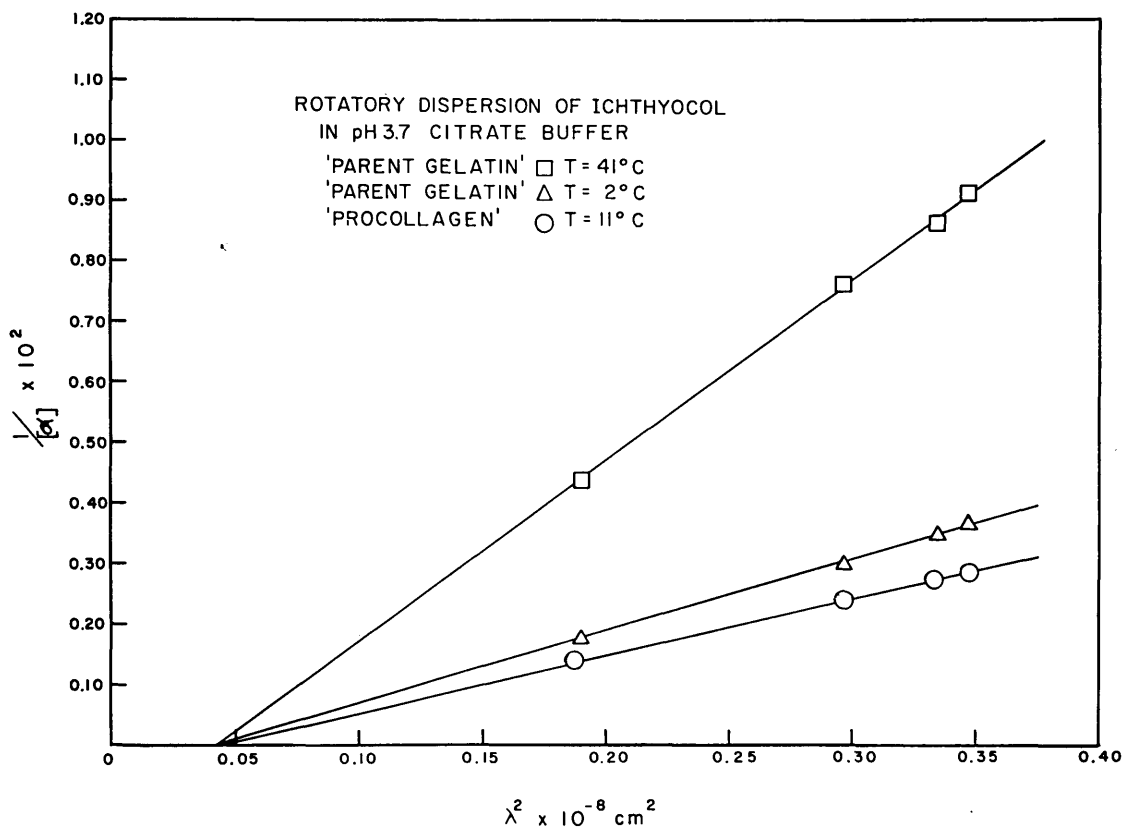


Figure 24

Table 6

Representative Specific Rotation Values

	λ m μ				
	436	546	578	589	
$[\alpha]^{11^\circ}$	714	410	364	350	+8%*
$[\alpha]^{41^\circ}$	227	132	116	110	+13%
$[\alpha]^{2^\circ}$	570	331	289	276	+10%

* These % errors refer to the medium concentration range.

Table 7

Representative Rotatory Dispersion Constants

$$k = [\alpha]_{\lambda}^T (\lambda^2 - \lambda_0^2)$$

$$\text{assuming } \lambda_0^2 = 0.042 \times 10^{-8} \text{ cm}^2$$

		$\lambda^2 \times 10^{-8} \text{ cm}^2$		
	0.19	0.298	0.334	0.347
k_{11°	106	105	106	107
k_{41°	33.6	33.8	33.9	33.6
k_{2°	84.4	84.7	84.4	84.2

stant, the rotation constants obtained for these values are $T = 11^\circ \text{C.}$, $k = 106$; $T = 40^\circ \text{C.}$, $k = 34$; $T = 2^\circ \text{C.}$, $k = 84$. Table 7 gives this information. A value of $\lambda_0 = 0.042 \pm 0.006 \times 10^{-8} \text{ cm}^2$ (uncertainty estimated) is indicated by the data of Figures 21, 22, and 23.

Only the 'parent gelatin' at 2°C. shows a significant concentration dependence. This was about 30% for the concentration range investigated (% refers to $\frac{[\alpha]_{c_1} - [\alpha]_{c_2}}{[\alpha]_{c_2}} \times 100$, where c_1 and c_2 are the highest and lowest concentrations tested). The experimental error is at least 10% for the lower concentrations so that one cannot derive the shape of the concentration dependence curve from these data.

4. The concentration dependence

An experiment was designed to check the reproducibility of the concentration dependence of rotation exhibited by 'parent gelatin' gel. A series of dilutions from one stock solution of ichthyocol 'procollagen' was made up. Three different concentrations of the 'procollagen' were heated to 40°C. for 50 minutes, then cooled to room temperature and placed in the polarimeter tubes. The tubes were carefully sealed by parafilm covered rubber stoppers. Water close to 0°C. was circulated through the tubes for 10 hours before readings were taken. Data from nine concentrations were obtained. A plot of the readings for $[\alpha]_{546}^{10}$ vs. c is given in Figure 25. This shows about a 12% concentration dependence for 0.02% to 0.31% solutions. The order of magnitude involved in the concentration dependence is in agreement with the data of Robinson (1952) and Ferry and Eldridge (1949), who used higher concentrations (the lowest was 0.1%) and different kinds of gelatin.

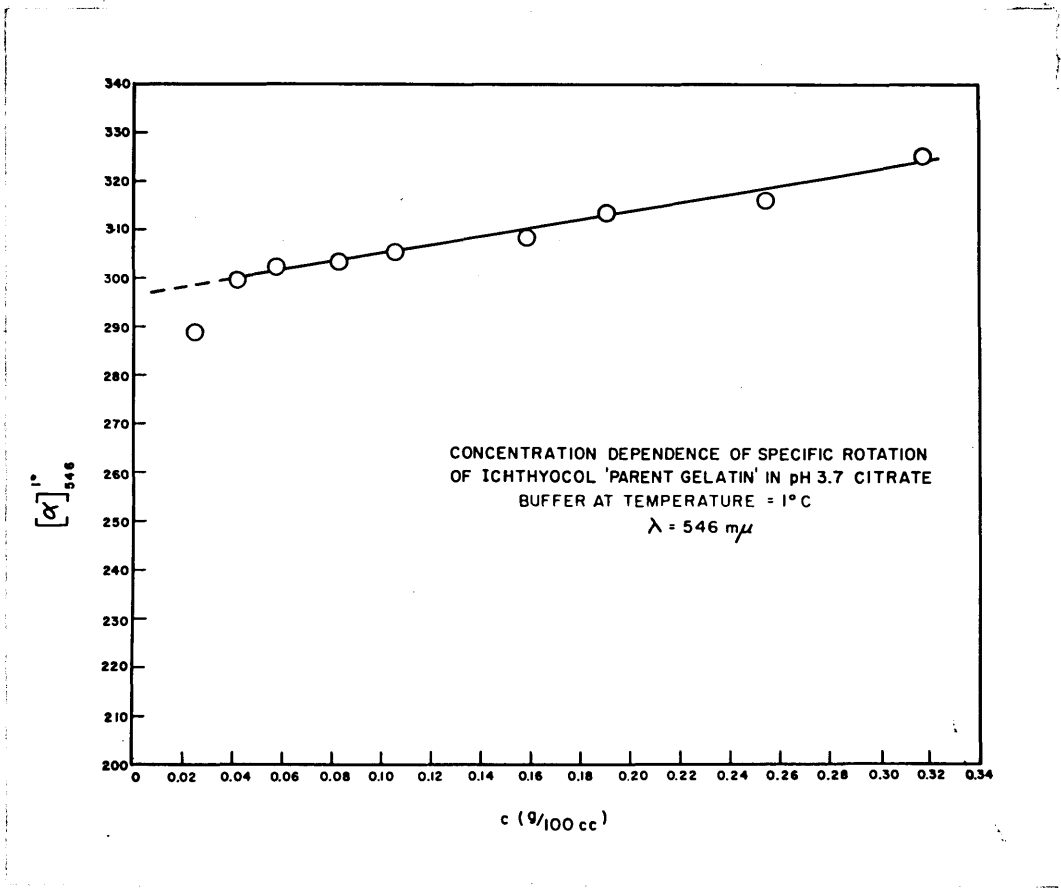


Figure 25

5. Dependence on ionic strength

A solution of ichthyocol 'procollagen' in 0.05% (wt) HAc (pH about 3.5) has a rotatory dispersion curve similar to that obtained for 'procollagen' in the higher ionic strength citrate buffer. This is true, also, for 'parent gelatin' at 40° C. at the two different ionic strengths. However, when the 'parent gelatin' is cooled, the rotations observed in 0.05% HAc do not reach values as high as those characteristic of cool 'parent gelatin' in citrate buffer. When $1/[\alpha]$

is plotted against λ^2 for this case, therefore, the slope is higher than that obtained with the 'parent gelatin' in citrate buffer. The extrapolation is to the same λ_0^2 in the two cases (see Figure 26 and compare with Figure 24).

That this is an effect of ionic strength is shown by the rotation of cold 'parent gelatin' in a solution of 0.05% HAc + 0.1 M NaCl. The specific rotation of this solution was similar to that of 'parent gelatin' in the citrate buffer. It may be noted that 'parent gelatin' in 0.05% HAc does not "gel" at concentrations where gelling occurs in higher ionic strength solutions.

6. Studies on films

Preliminary experiments were done on the rotatory dispersion of films prepared from 'parent gelatin.' These were made by dissolving ichthyocol 'procollagen' in 0.05% HAc, then heating the solution above 50° C., or by heating the 'procollagen' with distilled water. A known volume was then pipetted onto a cooled, circular optical flat, and this was transferred to a desiccator. The desiccator was then partially evacuated to speed up the drying process. The desiccator was placed

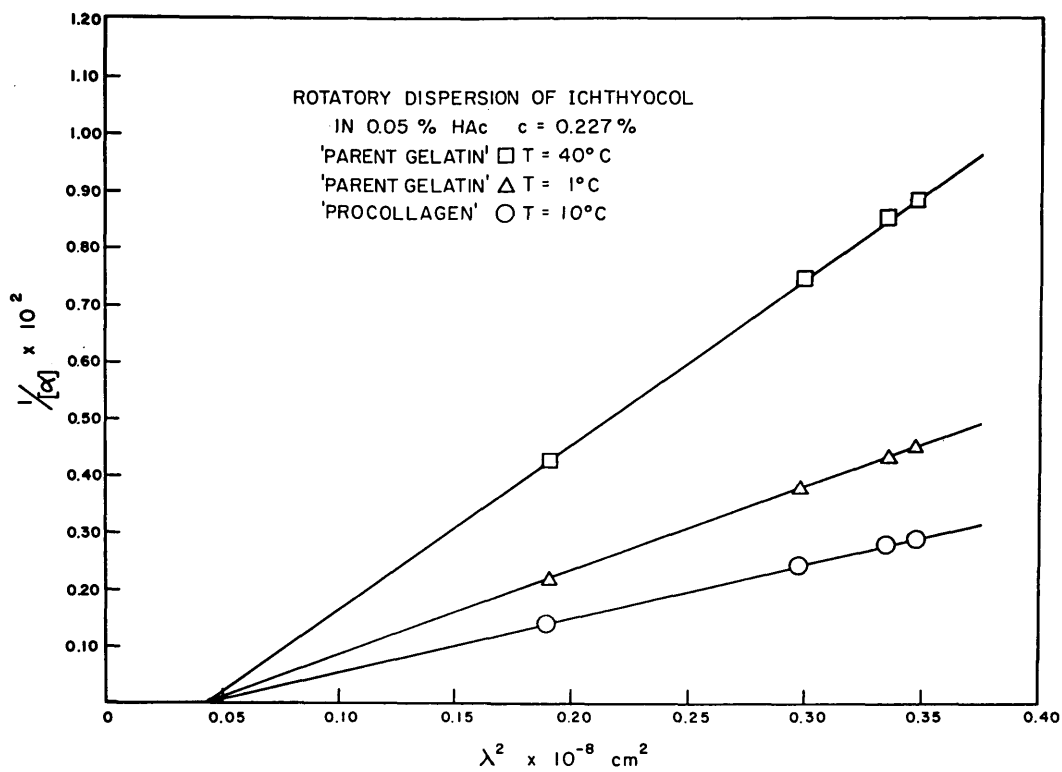


Figure 26

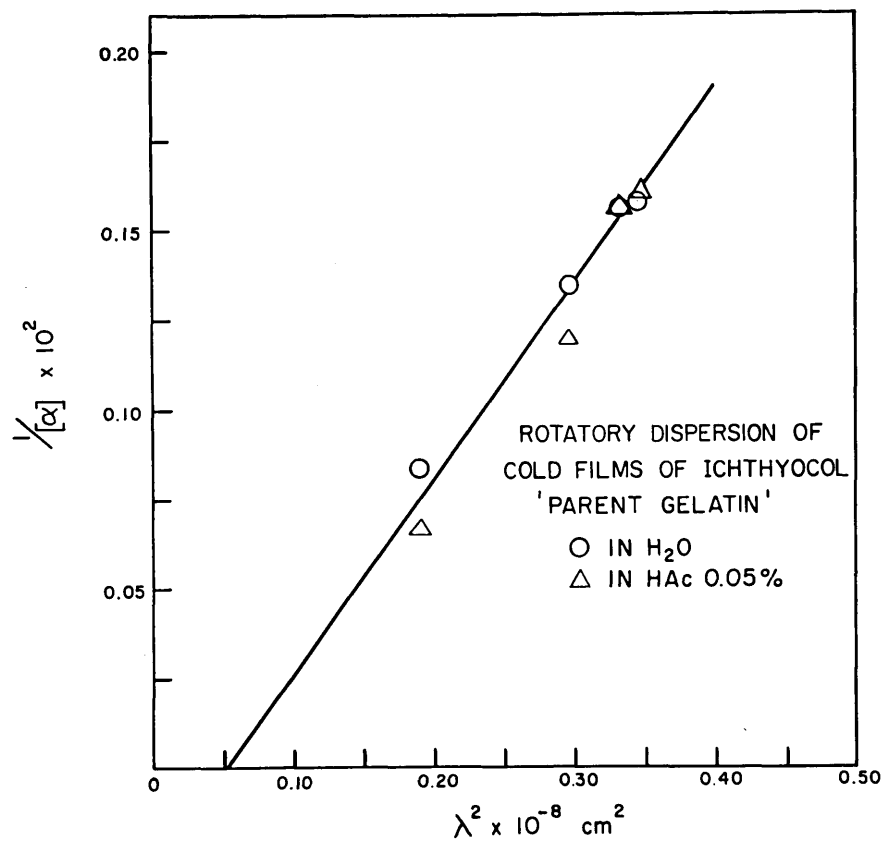


Figure 27

either in the refrigerator at about 4° C., or in the drying oven at about 60° C. In the former case, drying took about two days and in the latter, overnight.

One can determine the concentration of the original solution by using the Biuret reagent on a known dilution. From the number of grams of protein distributed over the area of the flat, one can calculate a film thickness which is probably accurate to about 25%. The optical flats to be examined were placed in a special holder to keep the surface of the film normal to the incident light in the polarimeter.

This was done for two kinds of film: one, made from a solution of 'parent gelatin' in distilled water, and having a thickness of 9μ ; and the other prepared from a solution of 'parent gelatin' in 0.05% HAc and having a thickness of 8.4μ . Two of the latter films were placed together for the rotation readings. Figure 27 shows the results for these films. $1/[\alpha]$ is plotted against λ^2 . It is clear that the values for the specific rotations are much higher than those obtained for 'procollagen' in solution (e.g. $k \approx 190$). Within experimental error a straight line is obtained by plotting the data in this way. No significant difference for the two kinds of film was observed. The rotatory dispersion constant for the films seems to be the same as that determined for solutions.

Because of the birefringence of the films and difficulties in determining film thickness, a more exact determination of the film rotativity was not made. Films prepared the same way, but dried in the oven at 60° C., had approximately the same film thickness as the cold 'films.' However, these 'hot' 'parent gelatin' films had rotations which were too low to be detected by the methods used. This is in

agreement with the results of Robinson (1953) who reported 'cold' gelatin films to have $[\alpha]_D \approx -1000^\circ$ and 'hot' gelatin films to have $[\alpha]_D \approx -125^\circ$.

Films of unheated 'procollagen' were prepared and dried in the refrigerator, but an osmotic effect caused salt accumulation in the center of the films, so that accurate readings could not be carried out. It appeared, however, that such films had a rotation comparable to the 'parent gelatin' films dried in the cold.

7. Summary of experimental data

1. The specific rotation of solutions of 'procollagen' from ichthyocol and calf hide (in citrate buffer, pH 3.7, 0.15 M citrate) is $[\alpha]_D^{10} = -350 \pm 30^\circ$. The solutions have an intrinsic viscosity of about 19 and 28 respectively.
2. Upon being converted to 'parent gelatin' by heating to 30° C. and greater, the solutions have rotations of $[\alpha]_D^{30} = -110 \pm 20^\circ$, and an intrinsic viscosity of 0.34 for the ichthyocol, and 0.4 to 0.6 for the hide.
3. In some cases, the decrease of rotation reaches completion more rapidly than the decrease of intrinsic viscosity.
4. 'Parent gelatin' solutions show a reversible mutarotation cycle with temperature, but upon cooling they do not reach a value of rotation as high as that characteristic of unheated 'procollagen' solutions ($[\alpha]_D^0 \approx -280^\circ$ for 'parent gelatin').
5. Ichthyocol 'procollagen' at 11° C., and 'parent gelatin' at 41° C. and at 2° C., show simple dispersion and have the same dispersion constant, within experimental error. Representative rotation

values for the medium concentration range give rotation constants for 'procollagen' $k_{11} = 106$, and for 'parent gelatin' $k_{41} = 34$, $k_2 = 84$, when a dispersion constant $\lambda_0^2 = 0.042 \times 10^{-8} \text{ cm}^2$ is assumed. A value of $\lambda_0^2 = 0.042 \pm 0.006 \times 10^{-8} \text{ cm}^2$ (uncertainty estimated) is indicated by the experimental data for the entire concentration range of 0.02% to 0.4%.

6. Specific rotations of ichthyocol 'procollagen' at 11°C. and 'parent gelatin' at 41°C. show little concentration dependence. The most marked concentration dependence is shown by 'parent gelatin' at 2°C. For the concentration range of about 0.02% to 0.3% this is about 12 to 30%.

7. A decrease of ionic strength at a pH of about 3.5 does not change the rotatory power of 'procollagen' at 11°C. or 'parent gelatin' at 40°C., but causes a decrease in rotation of 'parent gelatin' at 1°C. The rotation constant of the 'parent gelatin' at 1°C. is $k \approx 70$. The dispersion constant is unaffected for all the solutions by the change in ionic strength.

8. Films of ichthyocol 'parent gelatin' dried at about 4°C. have higher specific rotations than solutions of 'procollagen'. These films show $[\alpha]_D \approx -620^\circ$ and the rotation constant, k , is about 190. The dispersion constant is equal, within experimental error, to that of solutions of ichthyocol. Films of 'parent gelatin' dried at 60°C. have a very much lower specific rotation.

B. Discussion of experimental data

1. The conversion of 'procollagen' to 'parent gelatin'

Molecular interpretation of the optical rotation change: The bonds involved in this conversion would appear to be weak primary valence bonds, or secondary valence bonds such as hydrogen bonds, or van der Waal's

interaction forces. The peptide linkage should not be disrupted by the mild heat treatment used in the conversion process, hence secondary links are probably involved.

Bonds of this strength could be involved in three structural aspects of the 'procollagen' molecule: in the intermolecular lateral aggregation of the 'procollagen' molecules; in the end-to-end union of particles of 70,000 molecular weight to form the long 'procollagen' polymer; or in the internal polypeptide chain configuration of the 'procollagen' molecule. We will consider the possibility of relating each of these to the rotation change observed in the conversion to 'parent gelatin.'

Any intermolecular lateral aggregation in solutions of 'procollagen' would be disrupted by the heating process. However, the mass per unit length is reported by Gallop (1954) to be 80 - 120 avograms per A., which is in agreement with the specifications from x-ray diffraction for a single helical unit. Thus, the 'procollagen' molecule (under the experimental conditions reported) must be considered essentially a single long chain kinetic unit, and intermolecular lateral interactions are unlikely to be of significance for the optical rotation.

Since the end-to-end union of the 70,000 molecular weight particles is disrupted in the conversion process, this might be considered a possible source of the rotation change. However, the depolymerization corresponds roughly to the breakage of the 'procollagen' molecule in about ten places. Assuming a hypothetical four-chain model for the collagen protofibril, only eight terminal residues out of a total of about 700 would have the optical rotation changed in the

depolymerization process. Further, since the amide linkage may not be involved, the change in rotation, even of these residues, might not be very great. Therefore, we may consider that the depolymerization results in rotation changes which are negligible compared with the large decrease of rotation which occurs.

One is then led to attribute the rotativity behavior largely to changes in the internal configuration of the molecules which occur with heating.

The data correlating the viscosity and rotativity are in agreement with this point of view, since they indicate that different rates of reaction exist for the depolymerization and the optical rotation changes. These data may be interpreted as meaning that the internal configurational rearrangement is over before the depolymerization reaction reaches completion, the link connecting the units being stronger than the intra-unit bonds. For proper analysis of the kinetics, more exact temperature regulation is required.

The conclusion reached from this discussion is that the rotativity change occurring when 'procollagen' is degraded to form 'parent gelatin' is largely due to the change in internal configuration of the molecule making up the 'procollagen' polymer.

2. The mutarotation of 'parent gelatin'

The mutarotation phenomenon means that the 'parent gelatin' can reversibly regain much of the high rotation, characteristic of the 'procollagen.' This is shown very clearly by the rotation constants for 'procollagen' at 11° C., and for 'parent gelatin' at 41° C., and at 2° C. The cold 'parent gelatin' and the 'procollagen' solutions have k 's which are similar and quite different from that of the gelatin at 41° C.

In the introduction to this thesis, the two possible factors which might cause the mutarotation of gelatin were discussed. These are configuration changes and aggregation. Any interpretation of the mutarotation phenomenon amounts to an evaluation of the relative importance of these two factors.

The following discussion presents such an evaluation based on the experimental data reported in this thesis.

(a) The concentration dependence of mutarotation.

This is a case in which a conclusion is easily reached if large changes occur, but there is far more difficulty in interpreting a small change. That is, if the phenomenon of mutarotation had been greatly inhibited by decreasing the concentration of the gelatin solutions, then the conclusion that lateral aggregation is the more important factor would probably be valid.

However, the data presented above show that the effect amounts from about 10 to possibly 30% for the concentration range tested. This is small compared with the large change in rotation occurring as the solution is cooled. The concentration dependence does, however, seem to be larger than that found for the unheated 'procollagen' or for the 'parent gelatin' at 40° C.

A concentration effect on rotation has been found by investigators for many different kinds of molecules (for studies with proteins see Jirgensons, 1952b). Various theories, none of them convincing, have been advanced to explain this effect (Livens, 1913; Born, 1918; de Malleman, 1924). Thus, it is customary to express specific rotation as

$$[\alpha]_{\lambda} = \lim_{c \rightarrow 0} [\alpha]_{\lambda} + k'c$$

where $\lim_{c \rightarrow 0} [\alpha]_{\lambda}$ is the 'intrinsic' rotation of a system of molecules in which no interaction takes place, and k' is an empirically determined constant for the system.

According to the experiments described above, we would assign a small value to the interaction term and a large value to the configuration term. Since the cooled gelatin molecule is different from either the 'procollagen' or the gelatin sol molecule, the constant describing the concentration dependence could also be different.

Objections might be raised to this interpretation since aggregation was present even in the 0.02% solutions (Boëdtker, 1953). Significant changes of rotation, therefore, would not be observed until much lower concentrations were examined. This possibility cannot be neglected, nor can it be experimentally tested except by more refined means.

We may conclude then that the data from concentration dependence studies of mutarotation favor the configurational change as being more important than the aggregation effect.

(b) Interpretation of mutarotation

The preceding section has dealt with an experiment on gelatin in various states in an attempt to interpret a phenomenon which gelatin exhibits. Similar experiments have been described by other investigators (Ferry and Eldridge, 1949; Robinson, 1953). However, because of rotation studies on 'procollagen', a soluble, non-denatured collagen, a much more direct and convincing argument may now be given to explain the mutarotation. This is the following:

- (1) The decrease of rotation from -350° to -110° which occurs in solutions of 'procollagen' in the conversion to gelatin, has been shown in section 1. to be related only to the loss of the specific collagen configuration along the polypeptide chains.
- (2) Conversely, it must be expected that if the gelatin molecules can regain the collagen configuration, in part or completely, an increase of rotation up to a possible -350° is expected.
- (3) This does, in fact, occur when gelatin is cooled. There is proof from x-ray diffraction that the configuration characteristic of collagen is regained by at least parts of the molecule, and the rotation rises to values approaching -300° .
- (4) An additional point that aggregation per se does not produce this change of rotation is found in studies of gelatin films. Only the film having the specific collagen configuration showed the increase of rotation. Although there was maximum aggregation in the 'hot' gelatin film, no such increase occurred.

Therefore, we conclude that the mutarotation phenomenon in gelatin is largely to be correlated with the gain and loss of the specific collagen configuration.

Other experimental data are consistent with this interpretation. For example, the results of the experiment dealing with ionic strength, reported above, can be accounted for in the following way: the polypeptide chain configuration in the unheated 'procollagen' molecules in 0.05% HAc is well stabilized, and charge effects do not cause a configuration change. However, when 'parent gelatin' has been formed and the solutions are cooled, the charge effects at low ionic strength

impede the molecules from regaining the collagen configuration. This results in the relatively low laevorotation of cold 'parent gelatin' in 0.05% HAc. These charge effects are diminished by increasing ionic strength.

Various alkali halides, and urea, cause a large decrease in laevorotation (and viscosity) of gelatin 'gel' and a smaller change of rotation of the sol (Carpenter, 1927; Carpenter and Lovelace, 1935 a,b; 1938). These and similar reagents affect intramolecular linkages, particularly hydrogen bonds, stabilizing the collagen configuration, since they also cause thermal contraction in tendon (Gustavson, 1949). Both thermally contracted tendon and gelatin in the sol state show the 'amorphous' collagen wide-angle diagram in which the 2.86 A. reflection is missing. Thus, the decrease in laevorotation caused by these reagents may be associated with the loss of the collagen configuration in the gelatin molecules.

Although 'parent gelatin' can regain much of the collagen configuration, it does not regain all of it. This is seen from the different rotation constants of 106 and 84. Many of the differences between 'parent gelatin' and 'procollagen' are probably associated with this fact. Gelatin molecules have more loci available for intermolecular bonding than do 'procollagen' molecules. High solubility, aggregation and inability to reconstitute large spacings are therefore expected of such a system.

C. Conclusions

From the experimental data summarized on page 70, the decrease in rotation of $[\alpha]_D^{11} = -350^\circ$ to $[\alpha]_D^{30} = -110^\circ$, occurring when 'procollagen' is converted to 'parent gelatin,' is interpreted as

resulting from the loss of the specific collagen configuration within the 'procollagen' molecules. Accordingly, the mutarotation phenomenon exhibited by 'parent gelatin' is believed due for the most part to the gain and loss of the collagen configuration in the 'parent gelatin' molecules.

CHAPTER IV

Theories Relating the Rotatory Power and Configuration of ProteinsA. The correlation of rotatory power and helical configuration in collagen and gelatin.

The discussion in Chapter III was based on the fact that the configuration of the polypeptide chains in collagen was different from that in gelatin. No further specification of the configuration difference was made in the interpretation of the rotation data.

Robinson (1951,1953) has used similar experimental facts for gelatin (particularly the rotation correlated with infrared data for films) to attribute the mutarotation phenomenon to a configuration change. However, he denotes the collagen configuration as simply the specific collagen 'fold' and no precise atomic arrangement is specified.

The hypothesis is suggested here that it is precisely and solely the helical aspect of the collagen configuration, rather than any other kind of 'fold' which is responsible for the large rotation changes occurring in collagen and gelatin.

1. The argument

There are two possible sources of optical activity in a protein. One is due to side chains producing an asymmetry about the α carbon atom in the amino acid residues. The other is due to the configuration of the polypeptide chain backbone (C-O-N-C α). Thus, if a dissymmetric* configuration of the backbone were assumed by a

*A dissymmetric configuration is one which has no plane, center or alternating axis of symmetry. A dissymmetric configuration is not necessarily asymmetric. (See Partington, 1953)

polypeptide chain composed only of glycine residues, one would predict that the structure would be optically active. In proteins, the contribution of the backbone to optical activity is due both to its own symmetry properties and to its effect on the field about each asymmetric α carbon atom.

In general, one would not expect environmental effects alone to cause large changes in the optical rotation of proteins. We include in such environmental effects the influence of other solute molecules in the neighborhood (except when these are in extremely high concentrations). The α carbon atoms in the protein are usually separated from the environment by the side chains and they are not directly linked to the polar and conjugated groups on the side chains. Furthermore, any changes of rotation which might be produced by the environment would not be expected to be of the same sign for all residues, hence a partial cancellation would occur. These arguments apply also to those configuration changes in the backbone which, effectively, merely alter the environment about each α carbon.

The data on gelatin sols support this idea. Environmental changes such as pH and ionic strength have relatively little effect on the specific rotation (Kraemer and Fanselow, 1925; Carpenter, 1927; Carpenter and Lovelace, 1935 a, b). The small influence of intra- and intermolecular associations on rotation is seen from the fact that films made from gelatin sol have the same specific rotations as the solutions of gelatin sol (Robinson and Bott, 1951).

Certain backbone configurations are expected to have large values of optical rotation. A helix is such a configuration. The

optical rotation of a material depends upon the difference in its refractive indices for left and right circularly polarized light. A helix is a classical example of a dissymmetric structure which would be expected to show this refractive index difference (Kauzmann, Walter and Eyring, 1940). In a protein, the helical configuration of the polypeptide chains means that the backbone possesses this dissymmetry. In addition, the asymmetry about each α carbon atom might be changed by the helical configuration. Since the helix is composed of equivalent repetitive units (having one or more α carbon atoms) one would expect the same sign for the induced change of rotation in each unit. This might result in a large contribution to rotation. It may be noted, however, that the rotation due to the dissymmetry of the backbone is not necessarily of the same sign as that due to the asymmetry of individual amino acids.

The production of optical rotation by a helical configuration made up of symmetrical molecules is seen in quartz. Quartz is optically active only in the crystalline state when the SiO_2 molecules form helices (Lowry, 1935). An example in which the effect of the helix is superimposed on the rotation due to the asymmetric carbon atoms is seen in synthetic polypeptides. Co-polymers of γ -methyl-L-glutamate and DL phenylalanine show a change in specific rotation from $[\alpha]_D^{25} = -20^\circ$ to $+70^\circ$, as the percentage of α (hence helical) configuration rises from 15 to 100 % (Robinson and Bott, 1951).

The x-ray data interpreted in Chapter II of this thesis have shown that at least part of the collagen protofibril (corres-

ponding to the interbands) has a helical configuration. This configuration would certainly be maintained along some of the length of the molecule when collagen is dispersed in solution. Furthermore, it was shown in Chapter II that the large number of imino residues in collagen present a special stereochemical problem. That is, such residues may be incorporated more easily in either a right or a left-handed helix, depending upon the particular configuration. Thus, in collagen one would expect that the sense of twist assumed by the helix would be the one which could more easily accommodate the proline and hydroxyproline residues. There is then a possible reason for the presence of helices of one sense of twist in collagen.

We suggest, therefore, that it is this helical configuration of the polypeptide chains in at least part of the 'procollagen' molecules which is responsible for the high rotation. Hence, it is the gain and loss of this helical configuration which gives rise to large changes in rotation observed in collagen and gelatin.

2. Consequences of the theory

Having suggested the concept that the high rotations found under certain conditions in collagen are due to the helical configuration of the polypeptide chains, we can use the value of the rotation as a measure of this helical configuration. Specific rotations are here referred to the Na D line.

a. A specific rotation of about -110° might be that for a collagen molecule with little helical configuration, that is, a randomly coiled, or possibly β type of array of the amino acids. This occurs in the gelatin sol.

It is also possible that the value -110° characterizes gelatin molecules in which some of the helical configuration still exists, and a lower rotation would then be expected for completely random type of chain configuration. The effect of very high concentrations of certain salts such as KI (Carpenter and Lovelace, 1935 a,b) in decreasing the specific rotation of a gelatin sol below values of -110° might be related to this point. However, since high concentrations of urea cause an increase in the rotation of gelatin sols (Carpenter and Lovelace, 1938) the mechanism of these salt effects is not yet understood.

b. Specific rotations of -250° to -350° characterize a state of the protofibril interband in which at least some of the polypeptide chain is in a coiled configuration. Because of the much higher rotation in 'cold' films, one would suspect that the value -350° does not characterize the completely helical state of the interband.

c. Specific rotations of -620° to -1000° are found in high states of aggregation. One possibility is that these rotations correspond to a more highly coiled state of the polypeptide chain. When water is removed (as in the drying of a film), there would tend to be more intramolecular hydrogen bonding and thus a larger part of the polypeptide chain is likely to form the helical configuration.

A different explanation would be that interaction increases the contribution of already existing helices. The preceding discussion tends to support the first view.

3. Objections to the theory

Collagen and gelatin have a unique amino acid composition

due to the very large amounts of proline and hydroxyproline present. In the hypothesis outlined above, it was assumed that the significance of these residues for optical rotation is in causing the helices of collagen to have one sense of twist. However, the pyrrole ring in these amino acids involves the α carbon as one of its members. Strains in this ring might, therefore, have a large effect on the rotation of the α carbon. If the collagen configuration imposed such a strain, which was the same for all pyrrolidine residues, this might cause a very large total change in optical rotation. This objection is weakened, however, by the fact that the change in specific rotation from -100° to -350° for the protein would require a specific rotation of about -1200° for the proline and hydroxyproline residues. Furthermore, since there are two asymmetric carbon atoms in the hydroxyproline pyrrole ring, the change would have to be in the same direction for both, to produce a large effect. Therefore, until rotation data on proline and hydroxyproline in a variety of conditions is known, this argument cannot be evaluated.

B. An interpretation of the optical rotation of globular proteins.

In general, one should be cautious in extrapolating information about optical rotations from one system to another. However, in the case of proteins, this extrapolation may be justified for the following reason. Although very few rotatory dispersion investigations of proteins have been done, the data of Hewitt (1927) and Hansen (1927) for various globular proteins, including albumins and globulins, show dispersion constants in the general range of that of 'procollagen'. Since the theory here will be made for rotation values in the visible region of the spectrum, in particular the Na D line (589 m μ) small

differences in the dispersion constants in the ultraviolet region of the spectrum should not invalidate this comparison.

Two important facts are found in examining the data on globular proteins: (1) the specific rotations of native proteins are in the range of -30° to -60° (Jirgensons, 1952 a,b; Doty and Geiduchek, 1953). (2) Upon denaturation, the rotation rises and in some cases values up to -110° and -120° may be reached (Jirgensons, *ibid*; Kauzmann et al., 1953; Yang and Foster, 1954).

1. The denatured state

The hypothesis advanced here/ ^{to explain the above facts} is that upon denaturation globular proteins tend to approach a disordered, or randomly coiled, or β configuration of the polypeptide chains, and that a specific rotation of about $-100^{\circ} \pm 20^{\circ}$, characterizes this state. Thus rotations in the range of -80 to -120° would be expected for denatured proteins having an 'average'* amino acid composition.

At present, little evidence is available to test this hypothesis. In the following paragraphs the relevant data are summarized.

On the basis of a variety of experimental work, the concept has been developed that the 'denaturation' of globular proteins corresponds to some sort of unfolding or randomizing of the polypeptide chains (an important early reference is Mirsky and Pauling, 1936). Even in so-called reversible denaturation the large entropy changes involved (Kunitz, 1948) may imply a rearrangement of the polypeptide

*By 'average' we mean having a composition without a preponderant amount of any one amino acid.

chains toward a more probable, hence less specifically folded, configuration. Recent references on this point will be found in Anson (1953) and Lumry and Eyring (1954).

Two lines of evidence may be used to account for the rotation values of denatured proteins. One comes from the data on residue rotations of amino acids in positions where terminal effects are negligible. These have been measured for only a few amino acids. The data of Erlanger and Brand (see Erlanger and Brand, 1951, for references) show that in 0.5 N HCl, L-lysine has a specific rotation (as a residue) of -80° ; but L-alanine has a specific rotation of -246° . Until further evidence is accumulated for amino acid residues under varying conditions, the theory cannot be proved or disproved on this account.

Another line of evidence is provided by the rotation of proteins whose state is known to correspond to the randomly coiled or to the β configuration. The specific rotation of about -110° for gelatin sol may be cited as evidence. However, its unique amino acid composition (about 20% by weight of glycine and about 25% by weight of proline and hydroxyproline) may make the value -110° coincidental. The specific rotation of silk fibroin which is a β protein is of interest. The data of Coleman and Howitt (1947) show a rotation of about -60° for 'denatured' silk fibroin. However, since glycine makes up 42.4% of the nitrogen in this protein (Levy and Slobodiansky, 1949), the specific rotation for the same protein without glycine would be about -90° , which is in the range cited. The present author has found that the specific rotation of a solution of feather keratin, a β protein, dispersed in PO_4 buffer, is about -114° . This preparation was supplied by Mr. Malcolm Rougvie.

From the evidence cited, it is clear that the base line for an 'average' array of amino acids in a random or β configuration cannot yet be determined precisely, and there will certainly be a variation due to specific amino acid composition, but an average value of about -100° may not be far off if no very unique amino acid composition is involved.

2. The native state

A possible explanation of the specific rotation of native globular proteins is the following. The small negative rotations of these proteins (-30° to -60°) suggest that a large cancelling effect of some sort might be taking place, with the resultant low rotations observed due to an inequality in the cancellation. Such a situation would occur for example, if in globular proteins there were equal amounts of left- and right-handed helices made up of l-amino acid residues. The combined rotation of such helices might cancel to leave the small negative rotation actually observed.

An interesting point for this suggestion is the fact that the α helix which is favored as the structural basis for globular proteins (Pauling and Corey, 1953) has about equal probability of occurring in either a left- or a right-handed configuration so long as imino acids need not be incorporated into the coil (Crick, 1953 b; Pauling, 1953). Furthermore, since these residues do occur in relatively small amounts in globular proteins, they have been used to explain the 'turning of corners' in the structure (Pauling, 1940, 1953). In these positions, they would not determine the sense of twist formed by the rest of the helical backbone.

Accordingly, the increase of rotation observed upon denaturing a globular protein might be interpreted as resulting from a decrease in

the extent of well-ordered helical configurations in the polypeptide chains of the protein molecules.

It should be noted, however, that the helical configuration for globular proteins has not yet been proved, and the above argument could equally well have postulated some other configuration of the polypeptide chains, whose presence in a racemic mixture gives rise to a large cancelling effect.

C. Conclusions

1. An hypothesis is suggested that the large rotation values observed in collagen and gelatin are due to the helical configuration of the polypeptide chains along at least part of the protofibril. The mutarotation phenomenon exhibited in gelatin is therefore correlated with the gain and loss of the helical configuration of the polypeptide chains.

2. An hypothesis for the optical rotation values of globular proteins is the following:

The denatured state of globular proteins corresponds to a randomized or unfolded configuration of the polypeptide chains. A specific rotation of about -100° (depending on amino acid composition) characterizes such a state.

In the native state, globular proteins may have configurations where a large cancelling of optical rotation occurs. This would result in the low negative rotations actually observed. Such a situation would exist if globular proteins consisted of about equal numbers of helices having opposite senses of twist.

Summary

The main conclusions derived in this investigation are:

1. The polypeptide chains in collagen have a helical configuration in the portion of the protofibril which yields the wide-angle x-ray diffraction diagram.

2. The change of specific rotation which occurs when 'procollagen' is converted to 'parent gelatin' is due to the loss of a specific collagen configuration in the polypeptide chains of the 'procollagen' molecules. The mutarotation of gelatin is due to the gain and loss of this configuration within the gelatin molecules.

3. The preceding conclusions are correlated by an hypothesis which proposes that it is precisely the helical configuration of the polypeptide chains in portions of the protofibrils which is responsible for the high rotation values of 'procollagen.' Accordingly, it is the gain and loss of this helical configuration which produces the mutarotation in gelatin.

The evidence for these conclusions is summarized below.

1. A few observations were made using small-angle x-ray diffraction and electron microscopy, in addition to wide-angle diffraction, in order to add to information which indicates that all portions of the collagen fibril are not structurally equivalent.

a. Small-angle diagrams of tendon swollen in neutral salt solutions show the same alternating intensity relationship (odd orders strong and even orders weak) and loss of fanning, which previously had been known to occur in tendon moistened with distilled water.

b. Small-angle x-ray diagrams of dry tendon under high tension reveal for the first time that tension can produce the same effect as hydration, since the x-ray diagrams are similar to those obtained from hydrated tendon.

The evidence cited in a and b suggests that both water and tension increase interfibrillar orientation to permit the appearance of the cosinusoidal variation of electron density. Further, the disappearance of fanning and lengthening of the period indicate that this orientation takes place chiefly in the bands, or disordered regions of the fibril, which are located in both halves of the period.

c. A preparation of ichthyocol 'procollagen' can form fibrils with a 640 A. period, and 'segment long spacing' material with about an 1800 A. period. The polarimetric studies of this material, discussed below, therefore, relate to a 'typical' collagen system.

d. Wide-angle x-ray diagrams, which reveal small details of structure, were taken on the systems described above.

(1) Diagrams of moistened tendon or of dry tendon under tension show that no quantitative correlation can be made of the changes occurring at small and wide angles. This confirms previous ideas about the essential independence of results obtained at these two structural levels.

(2) Films of 'segment long spacing' ichthyocol 'procollagen' yield a poorly oriented collagen-type wide-angle diagram. This suggests that in the transformation to long-spacing material, some portions of the protofibril which yield the wide-angle diagram remain unchanged.

2. The part of the structure which the wide-angle x-ray diagram characterizes was shown to be helical by the following analysis:

a. Diagrams from dry tendon can be indexed according to a 28.6 Å meridional period for unstretched tendon, and about a 30 Å period for tendon under tension. The assignment of indices to reflections is the first step in the structure determination.

b. Patterns were obtained from moistened tendon under tension. These diagrams yield the intensity distribution expected from independently diffracting protofibrils.

This diagram was analyzed according to the theory of Cochran, Crick, and Vand (1952). In order to interpret the diagram in detail, a treatment was developed using 'helix-nets' (the mapping of cylindrical surfaces onto a plane). This treatment allows a simple presentation of helical diffraction ambiguities..

c. The collagen x-ray diagram is shown to be that of a helical diffractor. The genetic helix in the collagen protofibril has ten scattering nodes in three turns. The genetic helix is the simplest arrangement of equivalent scattering groups and does not necessarily show true chemical connections.

d. Further restrictions on the specific atomic arrangements of the polypeptide chains are derived. These are based on the x-ray diagram and chemical considerations.

3. Polarimetry was also used in this investigation since it is a sensitive indicator of short-range structural detail and permits analysis of material in solution.

For the first time a soluble, non-denatured, 'pure' collagen fraction, which had been characterized by physical-chemical methods (Gallop, 1953, 1954) was also studied by optical rotation. The following results were obtained:

a. Ichthyocol 'procollagen' in pH 3.7 citrate buffer has an intrinsic viscosity of about 20, and a specific rotation of $[\alpha]_D^{20} = -350 \pm 30^\circ$.

b. The 'parent gelatin' produced from the 'procollagen' by heating to temperatures greater than 30°C . has an intrinsic viscosity of about 0.34 and a specific rotation of $[\alpha]_D^{40} = -110 \pm 20^\circ$.

c. In some cases, in the conversion to 'parent gelatin', the decrease of rotation reaches completion more rapidly than the decrease of intrinsic viscosity.

d. The ichthyocol 'parent gelatin' (which has been characterized physico-chemically by Gallop (1953, 1954)) gels upon cooling and shows an increase of rotation $[\alpha]_D^0 \rightarrow -280^\circ$. The rotation change is reversible with temperature. This is the well-known mutarotation phenomenon of gelatin.

e. Similar results were obtained with 'procollagen' and 'parent gelatin' from calf hide.

f. Rotatory dispersion measurements reveal that ichthyocol 'procollagen' at 11°C ., and 'parent gelatin' at 41°C . and 2°C . show simple dispersion. That is,

$$[\alpha]_\lambda = \frac{k}{(\lambda^2 - \lambda_0^2)} \quad \begin{array}{l} k = \text{rotation constant} \\ \lambda_0^2 = \text{dispersion constant} \end{array}$$

The dispersion constant for all three temperatures is the same within experimental error.

Representative values for medium concentrations in the range 0.02 to 0.4 % yield $k_{11^\circ} = 106$, $k_{41^\circ} = 34$, and $k_{2^\circ} = 84$ assuming $\lambda_0^2 = 0.042 \times 10^{-8} \text{ cm}^2$. A value of $\lambda_0^2 = 0.042 \pm 0.006 \times 10^{-8} \text{ cm}^2$ (uncertainty estimated) is indicated by the experimental data in the entire concentration range investigated.

g. The concentration dependence is most marked for 'parent gelatin' at 2°C., and is 10 to 30% for the concentration range 0.02 to 0.3 %. This range includes concentrations lower than any reported in the literature, for polarimetric investigations of gelatin.

h. Preliminary investigations of the effect of ionic strength on rotation show that cool 'parent gelatin' has a lower specific rotation in solutions of 0.05 % HAc than in 0.15 M citrate buffer.

i. Films made from evaporating cold 'parent gelatin' have a very high rotation, ($[\alpha]_D^{25} -620^\circ$). Films made from evaporating hot 'parent gelatin' have a much lower rotation.

4. It is also suggested that globular proteins in the denatured state have a random or unfolded configuration of the polypeptide chains which may be characterized by a rotation of $[\alpha]_D^{25} -100^\circ$; and that in the native state they have a configuration in which a large cancellation of rotation occurs, resulting in the observed rotations of $[\alpha]_D^{25} = -30^\circ$ to -60° .

Suggestions for future work:

I. The x-ray diffraction analysis and structure determination

a. At present the most serious handicap in the structure determination of collagen is the lack of data on the amino acid sequence. The results of such an investigation would reveal the chemical significance of bands and interbands, and would enable a better estimate of the number of residues to be placed about each node of the collagen net. The frequency of the pyrrolidine residues would also be determined. The amino acid sequence should be carried out on a system such as 'parent gelatin' or some submit of this.

b. The stereochemical requirements of proline and hydroxyproline are as yet undetermined. Peptides with these residues should be studied crystallographically. This would reveal whether the cis- or transconfiguration of the peptide group occurred with these amino acids, and also whether the planarity of the peptide link is maintained.

c. The relation of the wide-angle pattern to the molecular structure of collagen must be clarified. In this connection, the diffuse reflections have to be correlated either with the portion of the helix backbone which gives the sharp near-meridional reflections, or to side chains, or to another part of the structure, perhaps the bands, having a different configuration from the interband backbone.

d. The properties of the collagen molecule, including size, are still not established. If the molecular weight of 'segmental long spacing' particles was found to be 70,000, the hypothesis of the extensibility of the 640 A. unit would be confirmed. If a unit of higher molecular weight were found, other molecular species in collagen would be indicated.

II. Optical rotation studies

a. On collagen and gelatin

More film work is necessary on 'unheated' 'procollagen' and on 'parent gelatin.' The rotation of tendon collagen should be determined. Comparative studies on 'procollagen' and 'parent gelatin' from other sources are also of interest. Gelatin solutions should be examined at higher temperatures to see whether there is more configurational change leading to a lower rotation. A further evaluation of the aggregation factor in mutarotation may be made by the addition to gelatin of reagents which inhibit aggregation. Katz and Wienhoven, (1933) examined the rotation of such systems, but a more refined analysis may now be made using combined light scattering and optical rotation data.

The particular role of proline and hydroxyproline in the rotation of collagen and gelatin has not yet been established. Rotation studies of these amino acids (as residues) under a variety of conditions should be made.

b. Other proteins

Much fundamental work on the optical rotation and rotatory dispersion of other proteins and synthetic polypeptides remains to be done. Synthetic polypeptides which can be transformed from the α to the β configuration should be analyzed both in solution and in films. The films could be correlated with x-ray diagrams. Since optical rotation is a most sensitive test of structural arrangement, G-F transformations of proteins, and both 'reversible' and 'irreversible' denaturation should be analyzed by this method. If fractionation of globular proteins is accomplished, as in the separation of the two kinds of chain in

insulin, the rotations of different fractions should be measured to see whether a difference in sign or size of rotation is found.

The eventual goal of such studies is a more precise correlation of configuration with optical rotation.

BIBLIOGRAPHY

- Ambrose, E.J., and Elliott, A. (1951). Proc.Roy.Soc.London A 206, 206.
- Anson, M.L. (1953) Les Proteines, Solvay, p.201.
- Astbury, W.T. (1940). J. Intern. Soc. Leather Trades Chemists 24, 69.
- Bear, R.S. (1942). J. Am. Chem. Soc. 64, 727.
- Bear, R.S. (1952). Advances in Protein Chem. VII, 69.
- Bear, R.S. (1954). Progress Report to the National Institutes of Health.
- Bear, R.S., and Cohen, G. (1952). Talk presented at meeting of American Crystallographic Association, Pa., June, 1952.
- Boedtker, H. (1953). Thesis, Radcliffe College, Harvard Univ., Cambridge, Mass.
- Boldman, O.E.A., and Bear, R.S. (1949). J. Applied Phys. 20, 983.
- Born, M. (1918). Ann. Physik 55, 177.
- Bowes, J.H., Elliott, R.G., and Moss, J.A. (1953). Nature and Structure of Collagen. ed. Randall, J.T. Academic Press, N.Y.p.199.
- Bowes, J.H., and Kenten, R.H. (1948). Biochem. J., 43, 358.
- Bragg, W.L., Kendrew, J.C., and Perutz, M.F. (1950). Proc. Roy. Soc. London A 203, 321.
- Bravais, L., and A. (1831). Ann. des Sciences Nat. 2, VII, 42.
- Bresler, S.E., Finoguenov, P.A., and Frenkel, S.I. (1950). Dokl. Akad. Nauk S.S.S.R., 72, 555.
- Brown, G.L., Kelly, F.C., and Watson, M. (1953) Nature and Structure of Collagen. ed. Randall, J.T. Academic Press, N.Y. p.117.
- Carpenter, D.C. (1927). J. Phys. Chem. 31, 1873.
- Carpenter, D.C., and Lovelace, F.E. (1935 a). J. Am. Chem. Soc. 57, 2337.
- Carpenter, D.C., and Lovelace, F.E. (1935 b). J. Am. Chem. Soc. 57, 2342.
- Carpenter, D.C., and Lovelace, F.E. (1938). J. Am. Chem. Soc. 60, 2289.
- Cochran, W., Crick, F.H.C., and Vand, G. (1952). Acta Cryst. 5, 581.
- Cohen, C., and Bear, R.S. (1953). J. Am. Chem. Soc. 75, 2783.

- Coleman, D., and Howitt, F.O. (1947). Proc. Roy. Soc. London A 190, 1943.
- Condon, E.V. (1937). Rev. Mod. Phys. 9, 432.
- Corey, R.B., and Pauling, L. (1953). Proc. Roy. Soc. London B 141, 10.
- Cowan, P.M., North, A.C.T., and Randall, J.T. (1953). Nature and Structure of Collagen, ed. Randall, J.T. Academic Press, N.Y., p.241.
- Crick, F.H.C. (1953 a). Acta Cryst. 6, 685.
- Crick, F.H.C. (1953 b). Acta Cryst. 6, 689.
- Crick, F.H.C. (1953 c). Thesis, Cambridge University, Cambridge, England.
- Crick, F.H.C. (1954). In press.
- Derksen, J.C. (1932). Collegium. 751, 838.
- Donohue, J. (1953). Proc. Natl. Acad. Sci. U.S. 39, 470.
- Doty, P., and Geiduschek, E. (1953). The Proteins IA, 393.
- Drude, P. (1900). Lehrbuch der Optik. Leipzig, 1900.
- Erlanger, B.F., and Brand, E. (1951). J. Am. Chem. Soc. 73, 4025.
- Ferry, J.D., and Eldridge, J.E. (1949). J. Phys. Chem. 53, 184.
- Fresnel, A. (1825). Ann. Chem. 28, 147.
- Gallop, P.M. (1953). Thesis, M.I.T., Cambridge, Mass.
- Gallop, P.M. (1954). In press.
- Gustavson, K.H. (1949). Advances in Protein Chem. 5, 354.
- Hansen, H. (1927). Compt. rend. Carlsberg. 16 #12.
- Hanson, A.W., Lipson, H., and Taylor, C.A. (1953). Proc. Roy. Soc. London A 218, 371.
- Hewitt, L.F. (1927). Biochem. J. 21, 216.
- Hudson, C.S. (1909). J. Am. Chem. Soc. 31, 66.
- Huggins, M.L. (1943). Chem. Revs. 32, 195.
- Jirgensons, B. (1950). Jour. Polymer. Sci. V, 179.
- Jirgensons, B. (1951). Jour. Polymer. Sci. VI, 477.

- Jirgensons, B. (1952 a). Arch. Biochem. and Biophys. 39, 261.
- Jirgensons, B. (1952 b). Arch. Biochem. and Biophys. 41, 333.
- Katz, J.R. (1932). Rec. trav. chim. 51, 835.
- Katz, J.R., and Derksen, J.C. (1932). Collegium, 752, 931.
- Katz, J.R., Derksen, J.C., and Bon, W.F. (1931). Rec. trav. chim. 50, 725.
- Katz, J.R., and Wienhoven, J.F. (1933). Rec. trav. chim. 52, 36, 385, 487.
- Kauzmann, W., and Simpson, R.B. (1953). J. Am. Chem. Soc. 75, 5154.
- Kauzmann, W., Walter, J., and Eyring, H. (1940). Chem. Revs. 26, 339.
- Kirkwood, J.G. (1937). J. Chem. Phys. 5, 479.
- Kraemer, E.O., and Fanselow, J.R. (1925). J. Phys. Chem. 29, 1169.
- Kuhn, W. (1930). Trans. Faraday Soc. 26, 266.
- Kunitz, M.J. (1948). J. Gen. Physiol. 32, 241.
- Küntzel, A. (1934). Collegium 1.
- Küntzel, A., and Pracke, F. (1933). Biochem. J. 267, 243.
- Livens, G.H. (1913). Phil. Mag. 25, 817.
- Levy, M., and Slobodiansky, E. (1949). Cold Spring Harbor S.Q.B. 14, 113.
- Lowry, T.M. (1935). Optical Rotatory Power. Longmans, Green and Co., London.
- Lowry, T.M., and Dickson, T.W. (1913). J. Chem. Soc. 103, 1067.
- Lowry, T.M., and Owen, G. (1930). Trans. Faraday Soc. 26, 371.
- Lumry, R., and Eyring, H. (1954). J. Phys. Chem. 58, 110.
- Malleman, de, R. (1924). Ann. de Physique 10 ser. 2, 1.
- Mirsky, A.E., and Pauling, L. (1936). Proc. Natl. Acad. Sci. U.S. 22, 439.
- Orekhovitch, V. N., Teustanovski, A.A., and Orekhovitch, K.D., and Plotnikova, N.E. (1948 a). Biochemistry, Leningr., 13, 55.

- Orekhovitch, V.N., Toustanovski, A.A., and Plotnikova, N.E. (1948 b)
Dokl. Aka. Nauk. S.S.S.R. 60, 837.
- Partington, J.R. (1953). Physico-chemical Optics. Longmans, Green
and Co., London.
- Pasteur, L. (1848). Compt. Rend. 26, 535.
- Pauling, L. (1940). J. Amer. Chem. Soc. 62, 2643.
- Pauling, L. (1953). Talk presented at the Conference on the Structure
of Proteins, Pasadena, September. (see Edsall, J.T. (1954).
Science, 119, 302.)
- Pauling, L., and Corey, R.B. (1950). J. Am. Chem. Soc. 72, 5349.
- Pauling, L., and Corey, R.B. (1951 a). Proc. Natl. Acad. Sci. U.S.
37, 235.
- Pauling, L., and Corey, R.B. (1951 b). Proc. Natl. Acad. Sci. U.S.
37, 272.
- Pauling, L., and Corey, R.B. (1953). Proc. Roy. Soc. London, B 141, 21.
- Pauling, L., Corey, R.B., and Branson, H.R. (1951). Proc. Natl. Acad.
Sci. U.S. 37, 205.
- Perutz, M.F. (1952). Annual Reports of the Chemical Society for 1951.
48, 362.
- Pomeroy, C.D., and Mitton, R.G. (1951). J. Soc. Leather Trades' Chemists,
35, 360.
- Randall, J.T., Fraser, R.D.B., Jackson, S., Martin, A.V.W., and
North, A.C.T. (1952). Nature 169, 1029.
- Robinson, C.R. (1953). Nature and Structure of Collagen. ed. Randall,
J.T. Academic Press, N.Y. p.96.
- Robinson, C.R., and Bott, M.J. (1951). Nature 168, 325.
- Rougvie, M., and Bear, R.S. (1953). J. Am. Leather Chem. Assoc.
XLVIII, 735.
- Schellman, J., Simpson, R.B., and Kauzmann, W. (1953). J. Am. Chem.
Soc. 75, 5152.
- Schmitt, F.O., Gross, J., and Highberger, J.H. (1953). Proc. Natl.
Acad. Sci. U.S. 39, 459.
- Schmitt, F.O., Hall, C.E., and Jakus, M.A. (1942). J. Cellular Comp.
Physiol. 20, 11.

- Simpson, R.B., and Kauzmann, W. (1953). J. Am. Chem. Soc. 75, 5139.
- Smith, C.R. (1919). J. Am. Chem. Soc. 41, 135.
- Tate, G.P., (1872). Proc. R.S.E. VII, 391.
- Thaureaux, J. (1945). Bull. Soc. Chim. Biol. 27, 327.
- Thompson, D.W. (1942). On Growth and Form. Cambridge Univ. Press, Cambridge, England.
- Trunkel, H. (1910). Biochem. Z. 26, 493.
- van't Hoff, J.H. (1875). La Chimie dans l'Espace. Rotterdam, 1875.
- Yang, J.T., and Foster, J.F. (1954). J. Am. Chem. Soc. 76, 1588.

APPENDIX I

Ambiguities of the Helical Diffraction Problem

A. The single-cell versus multiple-cell ambiguity

Consider two discontinuous helices superimposed in space. One is then held fixed and the other rotated about the common axis. As the angle of rotation increases, modulations appear in the transform for the single helix. Extinctions occur when the second helix is out of phase with the first by π radians. Similarly, when an n -fold rotation axis is coincident with the helical axis, a cable of n intertwining helices is generated. Because of the extinctions which occur in such a case, an ambiguity arises which is particularly important in interpreting helical diffraction patterns.

The development of this ambiguity may be illustrated by reference to a particular example. We begin with a discontinuous helix consisting of say ten nodes in three turns of a primitive helix. The single-cell net of this structure and the expected diffraction pattern are presented in Figure 1.

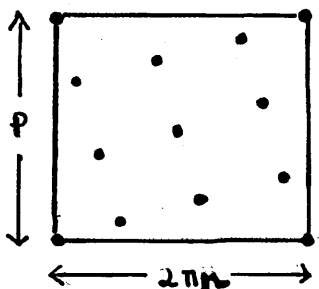


Figure 1a

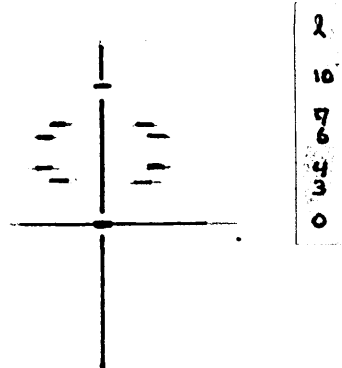


Figure 1b

We now place another identical helix π radians out of phase with the first and note the new net and the expected diffraction pattern (Figure 2).

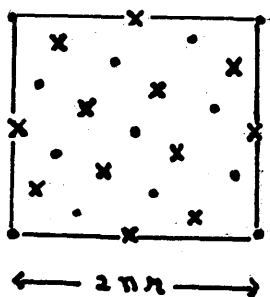


Figure 2a

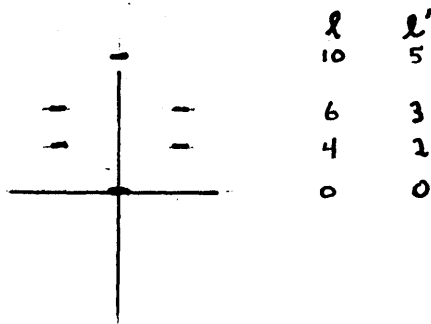


Figure 2b

It is clear that the pattern may now be indexed by $l' = l/2$; this corresponds, of course, to the halving of the period by the two-fold rotation axis. If this lower indexing is used, and the assumption is made that the strong near-meridional reflections observed correspond to J_1 Bessel functions and not J_2 's, a new single-cell net may be constructed which, when wrapped into a helix, would give rise to this same diffraction pattern (Figure 3).

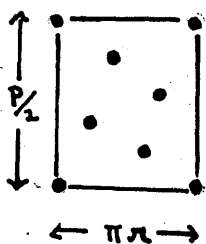


Figure 3a

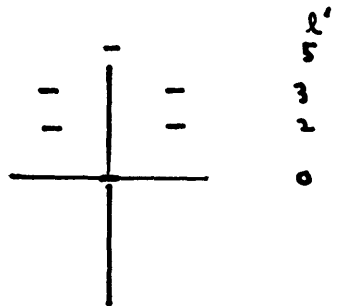


Figure 3b

This net has half the radius and half the nodes of the true compound net in Figure 2a (this is $\frac{1}{4}$ of the total number of nodes in Figure 2a). Conversely, we may consider that the two double-cell nets in Figure 2a correspond to a cable made up of four unit cells of Figure 3a. It will be shown that the transforms for the single-cell net of Figure 3a and the multiple-cell net of Figure 2a have the same form, but differ in the orders of Bessel functions and the radii involved.

By methods of this type, it is possible to prove that any cable made from helices related only by a rotation axis may be reduced to a simpler net. Conversely, if one takes the diffraction pattern as

the starting point, the analysis may be carried out most directly by drawing up the single simplest net which accounts for the lowest indexing of the pattern and then deriving the possible multiple-cell nets based on this.

It is instructive to prove the relation between the single-cell helix-net and the multiple-cell helix-net by a consideration of the transforms and the selection rules for the two cases. To do this we proceed as follows:

Consider a continuous cable of A helices related by a rotation axis coincident with the cable axis. The transform of this structure

is
$$T_c = \sum_{a=0}^{A-1} J_n(2\pi R a) \exp [in(\psi + \pi/2 - 2\pi a/A)]$$

$$= J_n(2\pi R a) \exp [in(\psi + \pi/2)] \left\{ e^{-2\pi n i} / e^{-2\pi n/A} \right\}$$

This last term is large only when

$$n = Aq, \text{ where } q \text{ is any integer.}$$

Selection rule (6) may be rewritten as

$$A(N_0/A)q = \lambda, \text{ where } n = Aq \text{ for each } \lambda. \tag{6a}$$

Thus the cable has the same period as the single-cell helix-net but is made of N_0/A turns. The transforms differ only in that the orders of the Bessel functions for the cable transforms are A multiples of those in the single-cell helix-net case, and the radii of the two are different.

This treatment may be extended to the discontinuous helix case. Here the same restriction on n will apply, namely only those values of n are permissible which are multiples of A . Thus equation (5) may be rewritten as

$$A(N/A)q = \lambda + Mm', \text{ where } n = Aq \text{ for each } \lambda. \tag{5c}$$

Equations (6a) and (5c) are then the most general cases.

When actual structures are considered and not the relation between the idealized single-cell helix-net and the derived cable, the relation $r_{cable} = Ar_{single-cell}$ will not, in general, hold. But since it is probable that the radius of the cable will be larger than that of a single helix, the radial positions of the diffraction maxima in reciprocal space may not be very different for the two cases.*

B. Connection ambiguities

Given a single-cell helix-net with an arrangement of nodes, various combinations of discontinuous helices may be derived which include all the nodes in the cell. The simplest case is that of the two primitive helices. Other possibilities include various kinds of cables. These cables may be composed of a single family of helices, all at the same radius from the central axis, or they may consist of any combination of helices from different families at different radii from the central axis. As in all connection ambiguity cases, only additional information, including detailed structure factors, will distinguish between some of the possibilities. Some examples of the problem follow.

- 1. The two solutions listed for the discontinuous helix (5a) and (5b) correspond to the existence in the net of two primitive helices. These two 'primitive' solutions have transforms which



* It may be mentioned that in the limit as $A \rightarrow \infty$ the cable approaches the net. The net-helix ambiguity (page 35) might be developed in this way.

differ only in the signs of the Bessel function terms ($n_1 = -n_2$). If there is cylindrical symmetry in the transform, i.e., if only one Bessel function term dominates the solution, they will have identical amplitudes in the transform.*

In the real structure, the node transform will be different for the two cases, and if the x-ray diagram is detailed enough, the correct solution may be selected.

2. Equations (7) and (8) point up the ambiguity in the discontinuous helix versus the continuous coiled-coil case. Here, again, actual structure factors will, of course, show the difference between the two, but certain other features may be considered also.

It is easy to show that internal symmetry in the sub-pattern surrounding meridional reflections is predicted for an ideal discontinuous helix, but that this is not necessarily true for the coiled-coil. Furthermore, the sub-pattern repeats identically in the discontinuous helix case, but this is not true for the continuous coiled-coil, since the J_s Bessel function factor will have a different weighting value at various layer lines along the meridian, although it is constant along each layer line. In practice, however, there is a difficulty in trying to use these differences to distinguish between the two cases. If the portion of reciprocal space under analysis corresponds to distances in the structure of the order of magnitude of the scattering centers, conclusions drawn from the

* In the case where the lowest node on the net cell is located midway between the two origins (i.e. a two-node cell) the primitive helices differ only in having opposite senses of twist. It can be shown that in the transform, for every J_n term there is a J_{-n} term. Thus the geometrical symmetry has its mathematical counterpart.

idealized representations are not reliable. At relatively small angles, however, these criteria might be useful.

In appendix III, the transform of a continuous coiled-coil for collagen has been calculated (Figure 6). This should be compared with the transform of the discontinuous helix based on the same net (p. 42, Figure 13).

C. The packing of helices

Single strand helices in which all loci are at equal radii from a central axis and which scatter independently of one another have periodicity imposed in one direction only, along the helix axis, and no order specified in a direction perpendicular to this. The transforms in such cases are confined to continuous layer lines. The addition of scattering material at different radii from the central axis, as discussed in the connection ambiguity, has the effect of modulating the intensities. It is clear that additional packing arrangements which affect the transform by introducing extinctions complicate the task of elucidating the individual helical configuration. We may note some kinds of packing with suggested methods for analysis.

In the preceding section on net ambiguities one situation was examined in detail. In this case, helices are intertwined about one another so that they are operated on by a rotation axis coincident with the helical axis, an n -fold axis thus forming a cable of n intertwining helices. It was shown that the preliminary analysis can be done by considering the structure in terms of single-cell nets and derivative multiple-cell nets. Any pattern has an ambiguity of

interpretation based on this problem.

A special case of this situation arises where a rotation axis is made coincident with the axis of the major coil in a coiled-coil, thus generating a coiled-coil cable. The simplest way to handle the transform is to derive that for a single coiled-coil in the appropriate configuration, and then to examine the phase factor and selection rule for the cable case. The nature of the particular selection rule involved will determine the change in the transform of the individual coiled-coil. This treatment has been applied by Crick (1953b) to a two- and three-strand cable of a particular configuration of coiled-coils. If this coiled-coil cable is a possible way of interpreting a given pattern, different systems of indexing must be tried. The approach by single-cell helix-nets and multiple-cell helix-nets is not easily applicable to this case.

Other packing arrangements involving screw axes can be handled similarly.

We may note that for the usual packing arrangement where the individual helices do not intertwine, but simply group together, one samples the continuous transform at appropriate lattice positions.

APPENDIX II

The Optical TransformerA. Theory

At certain stages in an x-ray diffraction structure analysis, it is necessary to determine the diffractions expected from a proposed or preliminary model. This is usually done by structure factor calculations which are simply the mathematical analogue of the diffraction process. However, since diffraction is a general property of waves, a physical analogue is^{also} available. A two dimensional representation of a model, made on the proper scale, can be used to diffract visible light waves like a grating. The resulting diffraction pattern is equivalent to the intensity distribution expected from the actual model in a section of reciprocal space corresponding to the particular projection used. This is the principle of the 'optical transformer.' A complete discussion of the theory is given by Hanson, Lipson and Taylor (1953).

We will consider here only one kind of projection. We begin with the usual structure factor formula. (The notation is the same as that on page 28)

$$F(R, \psi, z) \propto e^{i2\pi/\lambda [Rr \cos(\phi - \psi) + z_3]}$$

$$\psi = 0$$

$$F(R, 0, z) \propto e^{i2\pi/\lambda [Rr \cos \phi + z_3]}$$

but $r \cos \phi$ is simply the projection of the structure on a plane through the axis perpendicular to the direction of the incident beam.

If this projection is used the intensities obtained correspond to those in the plane through the origin of reciprocal space,

perpendicular to the incident beam. It is obvious that this simple projection is particularly useful for cylindrical diffractors or for helical diffractors whose transforms essentially have cylindrical symmetry. This is true for the discontinuous helix when only one Bessel function term dominates such near-meridional reflection. In such cases, this one section through reciprocal space gives the complete intensity distribution.

It is also clear that the optical transformer is most easily used, both in theory and practice, when the diffractions from an individual unit only, without superimposed lattice, are to be examined.

B. Description and use of apparatus

The optical transformer used was designed and constructed by Mr. Harold Wyckoff. The system consisted of a Hg arc whose radiation was filtered for the 546 line. Two lenses of focal length 4 and 2 meters were used. A diagram of the system with analogous parts of the x-ray diffraction system is given below. This is taken from Bear (1954). See Figure 4.

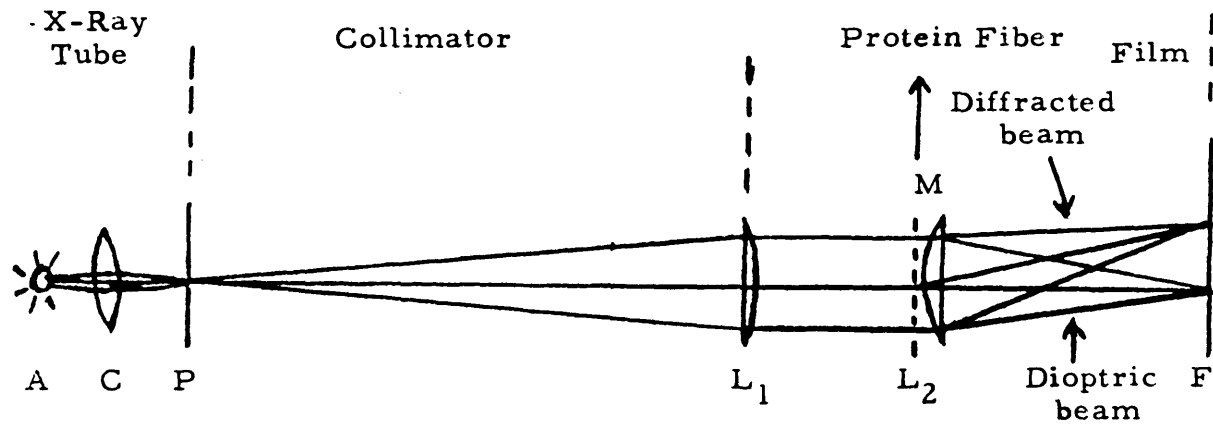
Model projections were made on the scale 1cm. equals 1 Å.

These were reduced photographically about 50 times to produce the final negative used as a mask. In order to reduce aberrations caused by imperfections on the gelatin surface of the negative, the mask was coated with an immersion oil which matched the refractive index of the gelatin. This was then placed between optical flats in a holder.

Exposure times varied depending upon the pinhole and masks used, but were generally less than one hour.

THE OPTICAL TRANSFORMER

Analogous parts of x-ray diffraction system:



- A = Hg arc
- C = Condensing lens
- P = Pinhole, acting as source for collimator
- L₁ = Collimating lens
- M¹ = Mask simulating structure
- L₂ = Lens focusing diffraction by mask
- F² = Film to register 'optical transform'

Figure 4

APPENDIX III

The Calculation of the Fourier Transform of the Continuous Coiled-Coil in Collagen

Crick(1953 a,b) has derived the expression for the Fourier transform of a coiled-coil and has used this to predict the meridional and near-meridional reflections expected from a model for α keratin. Since a very gradual coiling takes place in the major helix in this model, equation 2 in Table 3 may be used. Crick did not employ the formula to obtain either the relative positions or magnitudes of the reflections for each layer line.

We wish to use the transform to determine the intensities expected for a continuous coiled-coil model for the genetic helix in collagen. This calculation serves as a test for the 'optical transformer' described in Appendix II, and in addition furnishes more accurate intensity relationships than can be obtained by that method.

The genetic helix we are considering has ten turns of the minor coil in three turns of the major coil for the 30 A. period. It is apparent that equation 3 must be used here. This means that 4 Bessel functions are factors in each term. We may rewrite equation 3:

$$F(R, \psi, z/c) = \sum \sum \sum \sum J_p(2\pi R r_0) J_q(2\pi R r_1) J_s(2\pi(z/c) r_2 \sin \alpha) J_d(2\pi R \Delta) e^{i\phi}$$

where $\phi = p(\psi - \phi_0 + \pi/2) + q(-\psi + \phi_1 + \pi/2) + s(\phi_2 + \pi) + d(\psi + \phi_3 + \pi/2) + 2\pi z z_0/c$

We may take $\psi = \phi_0 = \phi_1 = z_0 = 0$,

from which we get

$$\phi = (p + q + d) \pi/2 + s \pi .$$

The implicit assumption of cylindrical symmetry which was made here can be proved correct for values of $R \leq 0.10$. Deviations from cylindrical symmetries are probably not very great for values of $R < 0.30$.

More than one term must be used for calculating the intensity at each point in reciprocal space even for near-meridional reflections. We wish to eliminate all terms but those which will have an appreciable value. To do this we consider each of the four Bessel function factors separately. Given a model with prescribed radii for the major and minor coils, the arguments of the J_p , J_q , and J_d factors will depend only on R , the radial coordinate in reciprocal space. For the specific example here, the following values were used:

$$r_0 = 2.4 \text{ \AA}, \quad r_1 = 1.80 \text{ \AA}, \quad C = 30 \text{ \AA}.$$

$$\Delta = 0.41 \quad \bar{r}_1 = 1.41$$

(Dimensions of the α helix were used for the minor coil)

Substituting these, we get:

$$J_p (15.1 R), \quad J_q (8.76 R), \quad J_d (2.54 R)$$

By plotting the values of different orders of these Bessel function factors, as a function of R , we can determine when they no longer have an appreciable value for the region of reciprocal space under consideration. Thus, the following table may be drawn up:

	$R = 0.10$	$R = 2 \sin \theta / \lambda$ 0.20	0.30
p	$0 \pm 1 \pm 2$	$0 \pm 1 \pm 2 \pm 3 \pm 4$	$0 \pm 1 \pm 2 \pm 3 \pm 4 \pm 5$
q	0 ± 1	$0 \pm 1 \pm 2$	$0 \pm 1 \pm 2 \pm 3$
d	0 ± 1	0 ± 1	$0 \pm 1 \pm 2$

The integers are the orders of the Bessel function factors which must be considered.

The argument of the J_s Bessel function factor depends only on layer line index and is constant over a given layer line for all radial positions. For the collagen case this is $J_s(0.32 \lambda)$. A similar plot is made for this factor and it turns out that values of from 0 to $\frac{1}{2} l$ must be considered at the tenth layer line. Fewer orders are necessary for layer lines of smaller index.

The next step is a consideration of the selection rules. It is necessary to determine the relative sense of twist in the major and minor coils since different selection rules occur for the two possibilities of the same or opposite sense of twist. It is easily shown that on layer lines which are integral multiples of λ/N_0 , identical solutions occur for the two cases (this is due to these layer lines exhibiting the continuous helix aspect of structure). For other layer lines the following relationship exists:

$$\begin{aligned} p_s &= p_{as} & q_s &= -q_{as} & s_s &= -s_{as} \\ d_s &= -d_{as} \end{aligned}$$

where the subscript 's' refers to the solution in which both helices have the same sense of twist, and the subscript 'as' to the one in which they have opposite senses of twist.

Using either one of the two possible selection rules the solution corresponding to the other selection rule can be immediately found by the above rules.

For the collagen case, calculations for both solutions were carried out up to values of $R = 0.10$ in reciprocal space. The solution which agreed better with the x-ray pattern was then chosen

and the calculation done for values of R up to 0.30. For the collagen case this turned out to be the one in which the major and minor helices had the same sense of twist.

The selection rule used was: $3p - 13q - 7d = 2 + 10s$.

A table was drawn up for possible combinations of $3p$, $13q$ and $7d$, in which all the permissible integers for p , q , and d were included. Inserting the value of s in the selection rule, all possible solutions were determined, and checked off by reference to this table.

For radial positions near $R = 0.30$, more than 30 terms in some cases had to be considered. In addition proper attention had to be paid to the sign of the Bessel function factors, as well as to the phase factor ϕ . However, once all the solutions were tabulated, corresponding to the permissible combinations of p , q , d , and s , the calculation was quite mechanical. The results were in excellent agreement with the diffraction pattern obtained using the optical transformer. A comparison of the calculated/observed intensities is shown in Figures 5 and 6.

It should be pointed out, that although the transform of the coiled-coil gives good agreement with the intensity distribution on the wide-angle diagram (see Figure 6), the coiled-coil model for collagen does not fulfill the necessary stereochemical requirements.

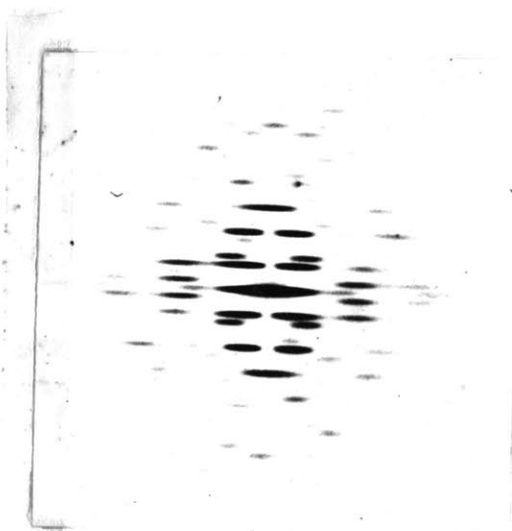


Figure 5a

Figure 5b

Projection of continuous coiled-coil for collagen and its optical diffraction pattern

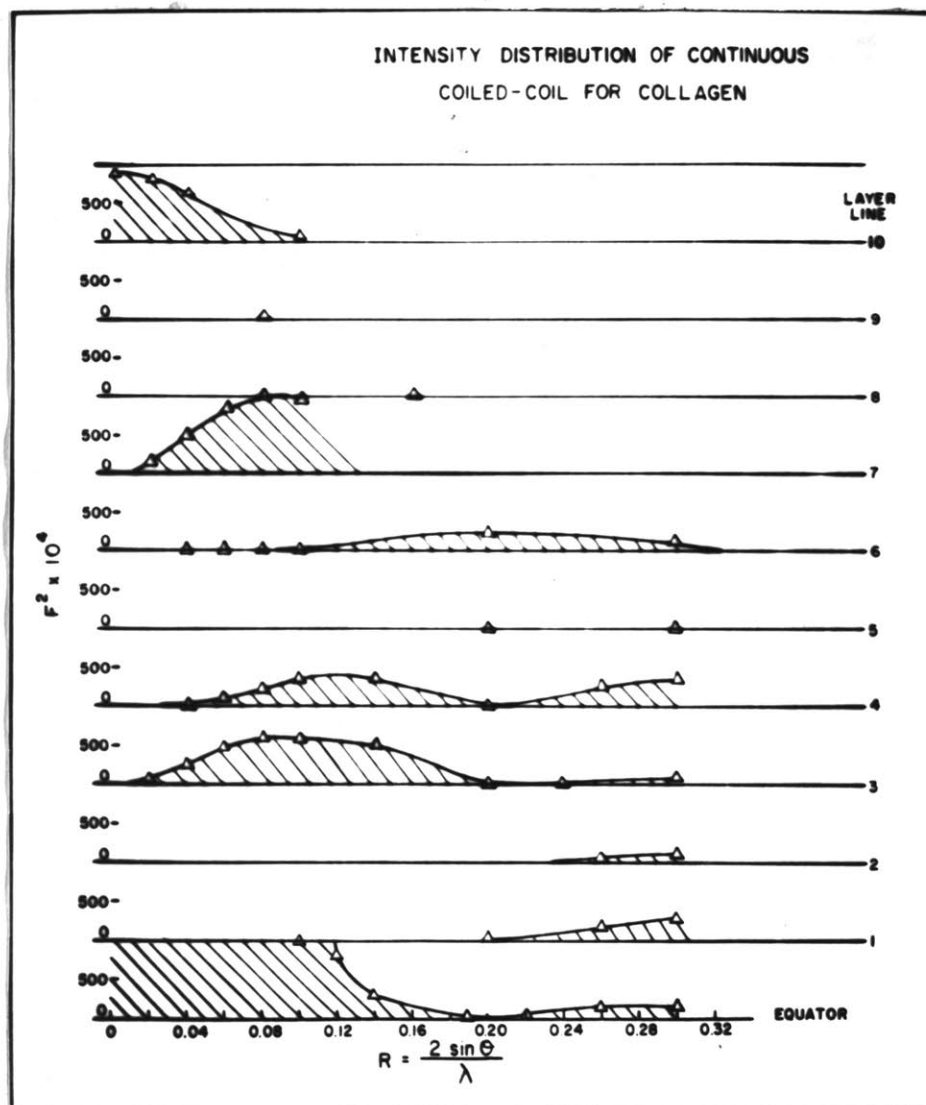


Figure 6

Biography

The author was born in Long Island City, New York, in June 1929. She attended the public schools of New York City, and was graduated from Hunter College High School. At Bryn Mawr College she majored in Biology and was graduated summa cum laude with Honors in Biology. In 1950 she entered the Biology Department at the Massachusetts Institute of Technology with an M.I.T. scholarship and as co-holder of the Bryn Mawr European Fellowship. During 1951-52 and 1953-54, she was research assistant in the Biology Department, and during 1952-53 was a predoctoral fellow of the National Science Foundation.